INL/RPT-23-71387

Cost Efficient-by-Design Microreactors

December 2022

Trade-offs between cost, technical, and regulatory factors

David Shropshire and Efe Kurt
Nuclear Science & Technology, Idaho National Laboratory

Alex Huning
Reactor Systems Modeling and Safety Analysis, Oak Ridge National Laboratory

Idaho National Laboratory

INL is a U.S. Department of Energy National Laboratory operated by Battelle Energy Alliance, LLC

INL/RPT-23-03080

Cost Efficient-by-Design Microreactors

Trade-offs between cost, technical, and regulatory factors

David Shropshire and Efe Kurt
Nuclear Science & Technology, Idaho National Laboratory

Alex Huning
Reactor Systems Modeling and Safety Analysis, Oak Ridge National Laboratory

December 2022

Idaho National Laboratory
Nuclear Science & Technology
Idaho Falls, Idaho 83415

http://www.inl.gov

Prepared for the
U.S. Department of Energy
Office of Nuclear Energy
Under DOE Idaho Operations Office
Contract DE-AC07-05ID14517

Page intentionally left blank

FOREWORD AND ACKNOWLEDGEMENTS

The present study was prepared under the Microreactor Program by David Shropshire and Efe Kurt from Idaho National Laboratory and Alex Huning from Oak Ridge National Laboratory. The authors wish to thank Chandrakanth Bolisetti, Jason Christensen, and Jorge Navarro for their insightful reviews and comments that improved the quality of the report.

Page intentionally left blank

ABSTRACT

This research evaluates a cost reduction investigation through adoption of a functional containment approach on the microreactor system and structure. Trade-offs between microreactor system designs, fuels and reactor module sizes are evaluated based on performance-based and risk-informed design procedures. Cost savings are evaluated against trade-offs in the reliability of passive heat removal systems, reactivity control, and radioactive material containment. Results can inform the Microreactor Program and reactor designs on "sweet spots" for microreactors that are cost-efficient while meeting required safety limits.

Page intentionally left blank

CONTENTS

FIGURES

TABLES

ACRONYMS

AOO	anticipated operational occurrences
DBA	Design Basis Accident
DBE	Design Basis Event
DID	Defense in Depth
DRACS	Direct Reactor Auxiliary Cooling System
EAB	exclusion area boundary
FP	fission product
F-C	Frequency Consequence
GCR	gas-cooled reactors
HALEU	High-Assay Low-Enriched Uranium
HP	heat pipe
INL	Idaho National Laboratory
IPyC	Inner Pyrolytic Carbon
LBE	Licensing Basis Event
LCOE	levelized cost of electricity
LMP	Licensing Modernization Project
LWR	light-water reactor
MSR	molten salt reactors
MST	mechanistic source term
MWe	Megawatt – Electric
MWt	Megawatt – Thermal
NGNP	next-generation nuclear plant
NRC	Nuclear Regulatory Commission
ORNL	Oak Ridge National Laboratory
OPyC	Outer pyrolytic carbon
PAG	protective action guidelines
PRA	probabilistic risk assessment
SFR	Sodium Fast Reactor
SiC	Silicon Carbide
SMR	small modular reactors
SSC	Structures, Systems, and Components
TICAP	technology inclusive content of application project
TI-RIPB	technology-inclusive, risk-informed, and performance-based

TRISO	tristructural isotropic

1. INTRODUCTION

Many of the current regulations have been written based on safety requirements of light-water reactor (LWR) technologies. They are mostly prescriptive and deterministic, for example, minimum wall thickness (~15 in.) to withstand the effects of natural phenomena (earthquakes, tornados) in reference to NUREG-800, Ch. 3. The Nuclear Regulatory Commission (NRC) staff paper for advanced reactors provides flexibility in the design as long as each safety barrier's performance for preventing radioactive material release is met (NRC 2018). This concept is referred to as the "functional containment." Functional containment refers to the set of barriers that, when taken together, effectively limit the physical transport of radioactive materials to the environment. Functional containment includes both physical structures, like a leak-tight containment or reactor building, but also other barriers designed to prevent any release of radioactive material to the environment, such as fuels (e.g., tri-structural isotropic [TRISO] fuel).

Functional containment was recently approved by the NRC for use by license applicants (NRC 2018). Gas-cooled and sodium-cooled reactors historically follow a functional containment approach for performing the radionuclide retention fundamental safety function while eliminating the need for large leak-tight LWR-style containment structures. Figure 1 illustrates how functional containment performance criteria can be applied to physical buildings, as needed for specific events.

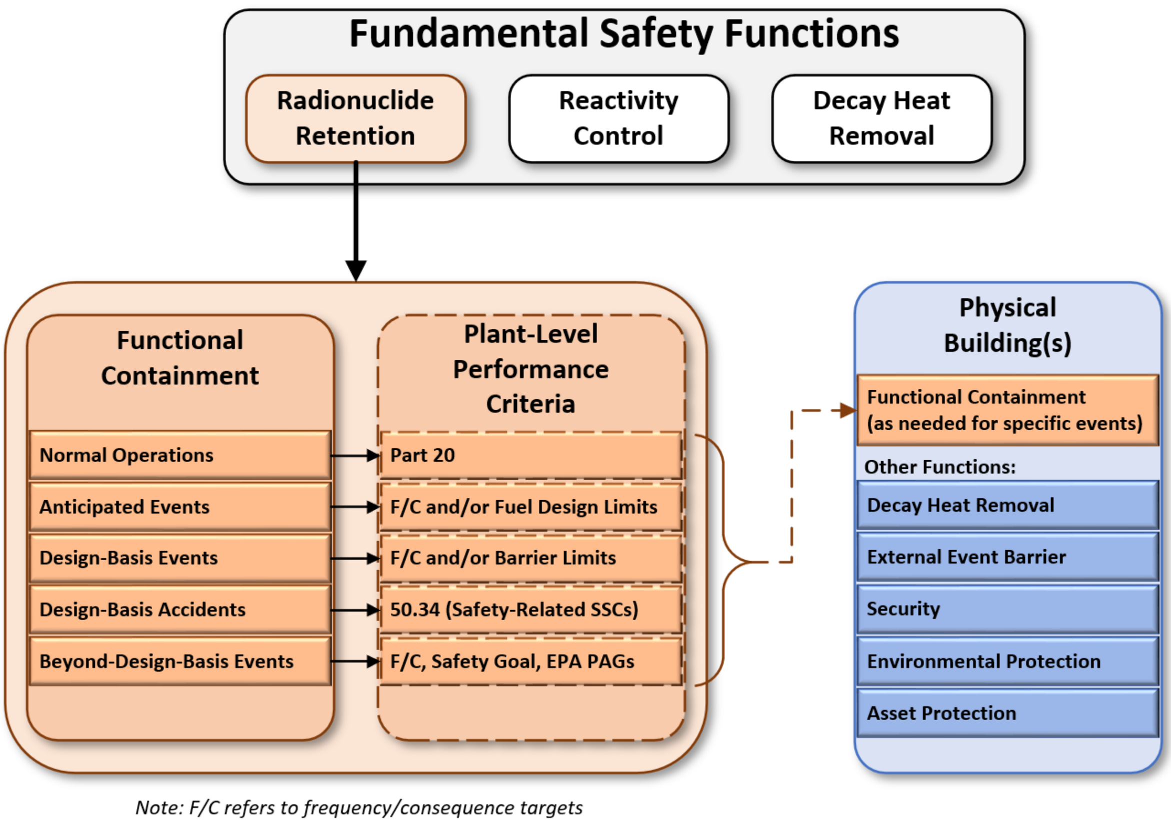

Figure 1. Functional Containment Performance Criteria (adopted from NRC 2018).

The design philosophy through functional containment design is based on a technology-inclusive, risk-informed, and performance-based (TI-RIPB) approach that:

1. Establishes objective criteria for evaluating performance

2. Develops measurable or calculable parameters for monitoring system and licensee performance
3. Provides flexibility to determine how to meet the established performance criteria in a way that will encourage and reward improved outcomes
4. Focuses on the results as the primary basis for regulatory decision making.

The risk insights from a probabilistic risk analysis (PRA) also form the basis for identifying and setting up decisions regarding anticipated operational occurrences, design-basis events, and beyond-design events.

1.1 Study Concept

A representative reactor system size scaling with different power levels is portrayed in Figure 2. Microreactors are relatively small in size and output capacity, generally less than 50 MWt. The reactor systems can be classified as microreactors, small modular reactors (SMRs), large-scale SMRs, and large power reactors that are above 500 MWt capacity. The scope of this work covers the microreactor size reactors, either as single units or a collection of units. The microreactors have a variety of possible core technologies including gas-cooled reactors (GCRs), molten salt reactors (MSRs), and heat pipe (HP) reactors. These microreactors have different fuel barrier systems, fuel release characteristics and fractions, primary barriers, and reactor buildings, if applicable. Depending on the technology chosen and the scale of the reactor, a combination of barriers, systems, components, and structures are necessary to satisfy associated safety, functional, and operational requirements.

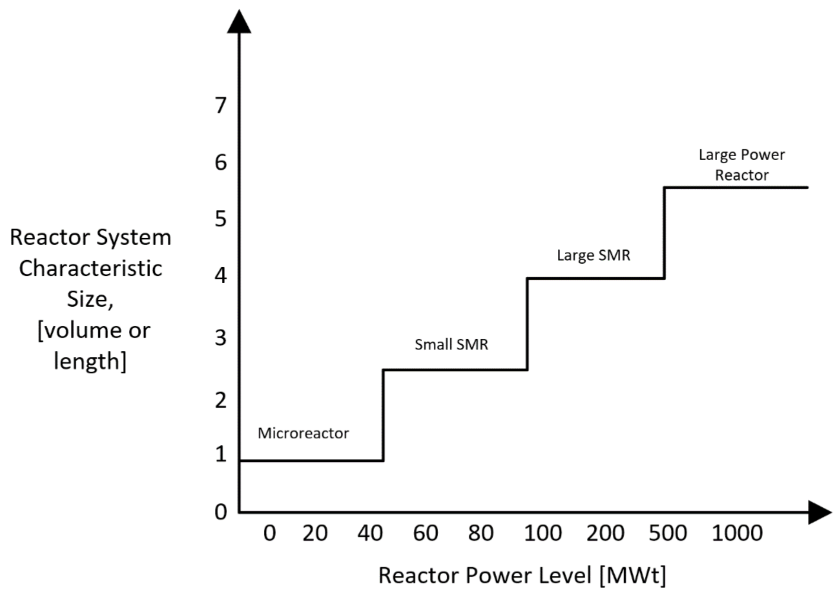

Figure 2. Example reactor system size scaling with power level.

For all events—normal operation through beyond-design-basis events—radionuclide release safety limits are established. For any specific event within those event categories, the barriers employed (i.e., the fuel, cladding, primary system, buildings and containment) must demonstrate that potential releases are within the acceptable limits. The economic benefits are clear for systems that meet all safety limits without employing overly conservative margins.

Functional containment is especially relevant as the initial source term, or radionuclide inventory, is increased for economic optimization, which then increases the required functional containment performance of all the barriers. This gives the designer the challenge to achieve the highest power output while minimizing the cost of the barriers. Microreactors sited near population centers or embedded with industrial applications may have a significantly reduced exclusion area boundary (EAB). This could potentially result in higher offsite dose consequences. The trade-off is to maximize the power output [maximum of 50 MWt] while achieving acceptable barrier performance at the least cost. Therefore, optimizations in the design may allow for a "sweet spot," that are cost-efficient while meeting all required safety limits. For example, a microreactor with a reference design of 20 MWt could be increased in power to 40 MWt while still meeting safety limits. This concept is illustrated in Figure 3.

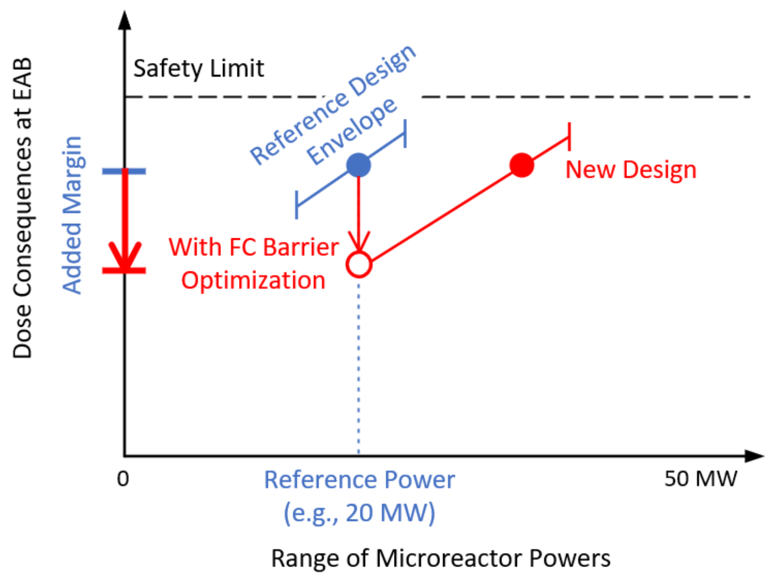

Figure 3. Design optimization with functional containment.

The reference microreactor design shown in Figure 3 is represented in terms of the dose consequence at the EAB for the worst-case accident and the power level that correlates with the radionuclide inventory to be contained within the system. For the reference or unoptimized case, the design should meet all safety limits, but radionuclide retention may be overly conservative with some barriers possibly being under-credited. With sufficient data and mechanistic source term analyses, barriers may be credited more effectively, allowing for additional safety margin. In turn, this could allow for a higher power level (as shown in Figure 3), or possibly fewer barriers, or a more flexible treatment of safety-related components.

The proposed methodology in Figure 4 shows application of the TI-RIPB approach for three different core designs including GCRs, MSRs, and sodium fast reactors (SFR). The risk insights from PRA and licensing basis events highly rely on the core technology. The safety features, defense-in-depth (DID), and safety classification of Structures, Systems, and Components (SSCs) are based on how their functional and safety requirements affect the outcomes of the frequency and consequence of events. Hypothetically, pushing the associated risk way below target or supporting performance curves that result in higher cost designs than needed to meet the required target curves. Risk is commonly defined using the "risk triplet" which is (1) a combination of what can go wrong, (2) how likely it to occur, and (3) what the consequences may be. Designers can iterate their design by selecting or introducing different safety features and the DID approach, which eventually affects the risk-informed cost. The approach employed in this study includes simplified case studies to communicate the concepts and relationships between key performance and risk variables, rather than producing absolute numbers.

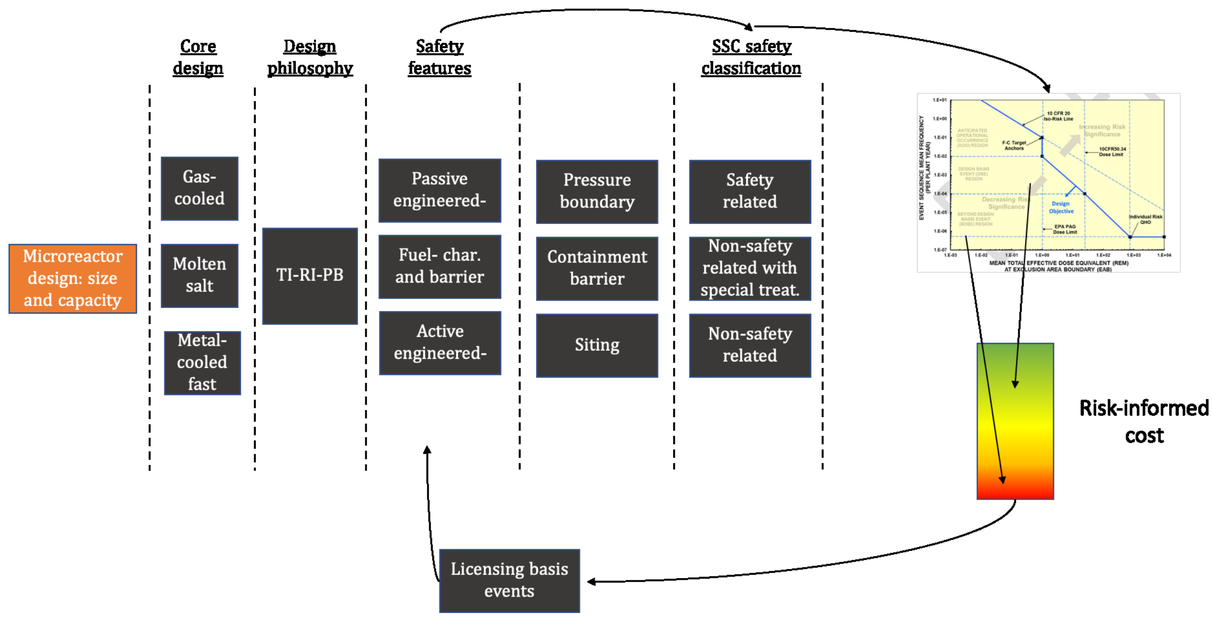

Figure 4. Proposed iterative TI-RIPB cost estimation for microreactors.

As an example of safety features, the TRISO fuel particle is an essential piece of the functional containment system proposed for use in GCRs. As shown in Figure 5, the TRISO fuel particle contains multiple layers of defense including Inner Pyrolytic Carbon (IPyC), Silicon Carbide (SiC), and Outer Pyrolytic Carbon (OPyC). These layers are intended to contain fission product releases in the event of a Design Basis Event (DBE), Design Basis Accident (DBA) and beyond DBE. These particles are extremely resistant to temperatures well above the normal operational temperatures of fuel particles (typically <1250°C). The TRISO particle has shown radionuclide retention for hundreds of hours at temperatures >1600°C without fuel particle failure and release. The large temperature margins enable two major aspects: (1) passive heat removal is independent of coolant pressurization, and (2) the greater use of negative temperature coefficients for intrinsic reactor shutdown. This means that a GCR with TRISO fuel is still able to remove heat without pressurization in the primary coolant boundary. This is critical in accident conditions as decay heat is still being removed even with a primary system break. Additionally, negative temperature coefficients encourage shutdown of the reactor (i.e., a negative reactivity coefficient) as temperatures increase. By retaining the radionuclides released during a DBE or DBA, the TRISO fuel particle coatings become the first layer of containment. A typical GCR may be designed without the conventional pressure-retaining containment structures, where the emphasis of radionuclide retention is at the source (i.e., at the fuel level).

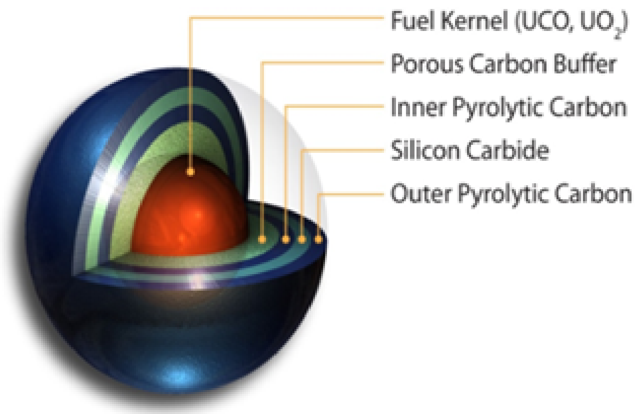

Figure 5. Schematic view of the layers of TRISO fuel particle.

Additionally, to reduce the cost and safety of advanced nuclear power plants at the system and component levels, several engineering options are being discussed including seismic isolators, deeply embedding reactor buildings, modular approaches, advanced concrete, etc. Seismic isolators can reduce the risks associated with microreactors at different siting locations and may provide the benefit of standardization against costly designs against seismic or shock wave events (Shropshire et al. 2021). Modular designs (Kurt et al. 2022), especially structural design of microreactors when needed, can be beneficial in terms of reducing the cost if they are not increasing the associated risks compared to alternatives. These include gaining direct labor work efficiencies including optimized labor use and coordination of trades, by building modules in a controlled environment, using equipment that can accurately duplicate operations, and using standardized shop processes and quality processes.

As stated above, this study develops the methodology to assess the benefits of the new regulations of functional containment, new fuel systems and potential systems, structures, and components on the economics of microreactors. The case studies discussed cover high-level radionuclide retention and consequences rather than conducting detailed PRA studies, which would be needed for licensing activities. The effects of the capacity of the microreactors and their impact on additional potential barriers are also discussed.

1.2 Regulatory Constraints and Conditions

The Licensing Modernization Project (LMP) led by Southern Company and cost-shared with the United States Department of Energy proposes changes to the LWR-based licensing approach for non-LWR technologies. Changes to the licensing approach include the highly integrated processes for PRA development (Moe and Afzali 2020a) licensing basis event (LBE) selection and evaluation (Moe and Afzali 2020b), SSC safety classification and performance targets, and evaluation of DID adequacy.

1.2.1 Safety Classification of SSC under the Licensing Modernization Project

Southern Company's SSC function safety classification process for achieving performance targets in the prevention and mitigation of LBEs is shown in Figure 6. (Southern Company, 2019a)

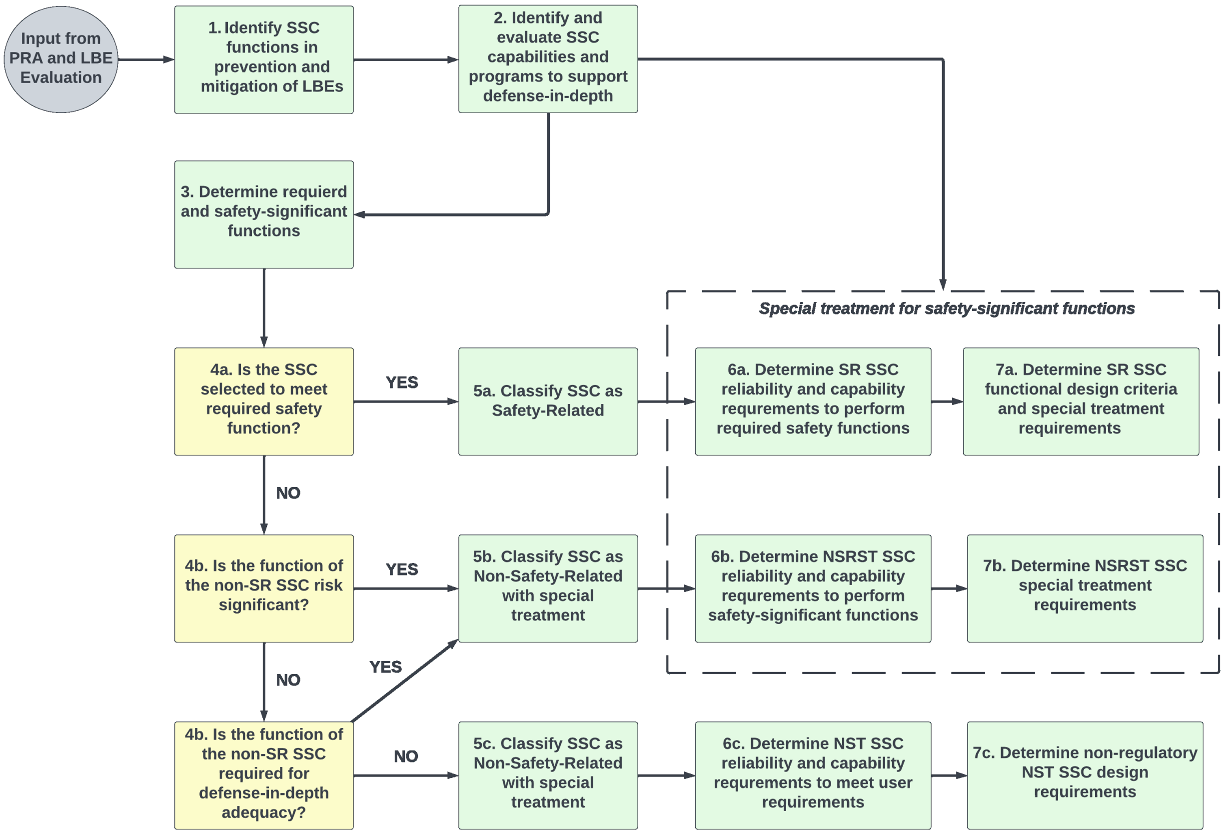

Figure 6. LMP SSC Function Safety Classification Process (regenerated from Safety Classification and Performance Criteria for SSCs).

The LMP methodology shown in Table 1 includes four SSC safety classification categories; safety-related (SR), non-safety-related with special treatment (NSRST), non-safety-related with no special treatment (NSRNST), and no special treatment (NST). SR SSCs are designed to perform the required safety functions to mitigate the consequences of DBE within the Frequency-Consequence (F-C) evaluation target. NSRST SSCs perform risk-significant functions to prevent any LBEs from exceeding the F-C target or contribute to the cumulative risk in the evaluation of total risk from all considered LBEs. NST SSCs have no special treatment required.

Table 1. Illustration of LMP methodology.

SSC Safety Classification Categories	Selected for Required Safety Function	Risk Significant	Required for DID	Relative Cost
Safety Related	✓	✓	✓	
Non-Safety-Related with Special Treatment	✓	×	✓	
Non-safety-related with no Special Treatment	✓	×	×	
No Special Treatment	×	×	×	

The South Texas Project (EPRI 2006) piloted exemption from special treatment requirements through the development a risk significance categorization process. This process included PRA, engineering judgment, and operational experience. Risk-information categorization of the SSC was done by an integrated decision-making panel. After risk-informed categorization, only 24% of the SR SSCs were categorized as safety significant. Seventy-six percent of those SR SSCs were categorized as low safety significant. Only 1% of the originally classified non-SR SSCs were subsequently categorized as safety significant, as shown in Figure 7.

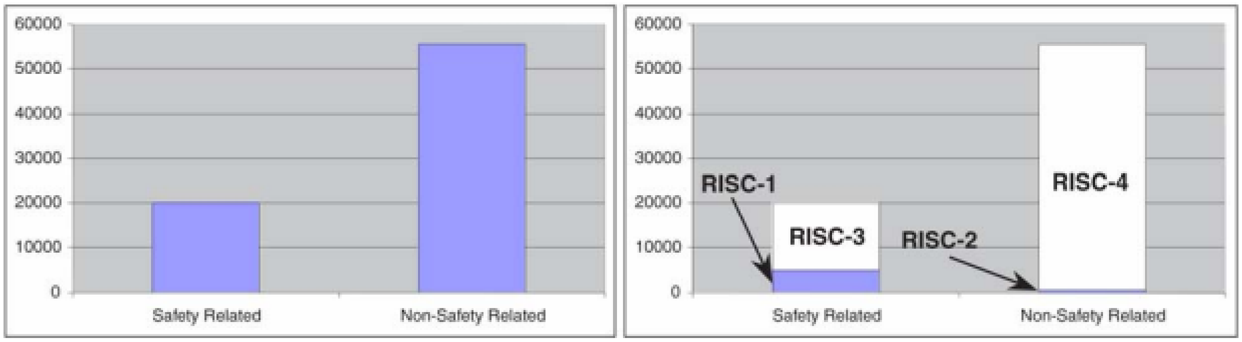

Figure 7. SSCs categorized under 10 CFR 50.69 for Texas Project.

Southern Company (2021) prepared a Technology Inclusive Content of Application Project (TICAP) licensing framework for developing content for specific portions of the NRC license application safety analysis report for non-LWR designs. Their approach included developing mechanistic source terms divided into:

1. Fuel performance and radionuclide transport in fuel particles and fuel pebbles up to the release of radionuclides from the surface of the fuel pebble into the surrounding gas space
2. Radionuclide transport phenomena outside of the fuel in the helium pressure boundary, reactor building, and the environment surrounding the outside of the reactor building.

Figure 8 shows the schematic for all major sources of radionuclide release from the fuel element. The classes of events initiating from radionuclide release from TRISO are as-fabricated defects, normal in-service releases, inert accidents, and oxidation accidents. The final barrier is shown as the reactor building in Figure 8. The Xe-100, unlike LWR technologies, does not need a pressure-retaining and leak-tight containment building (Southern Company 2021). Such containment building requirements compared to LWRs provides the opportunity to reduce cost and make the overall plant cost competitive. These capabilities, such as retention at the fuel level, provide the technical basis for a risk-informed and performance-based design approach.

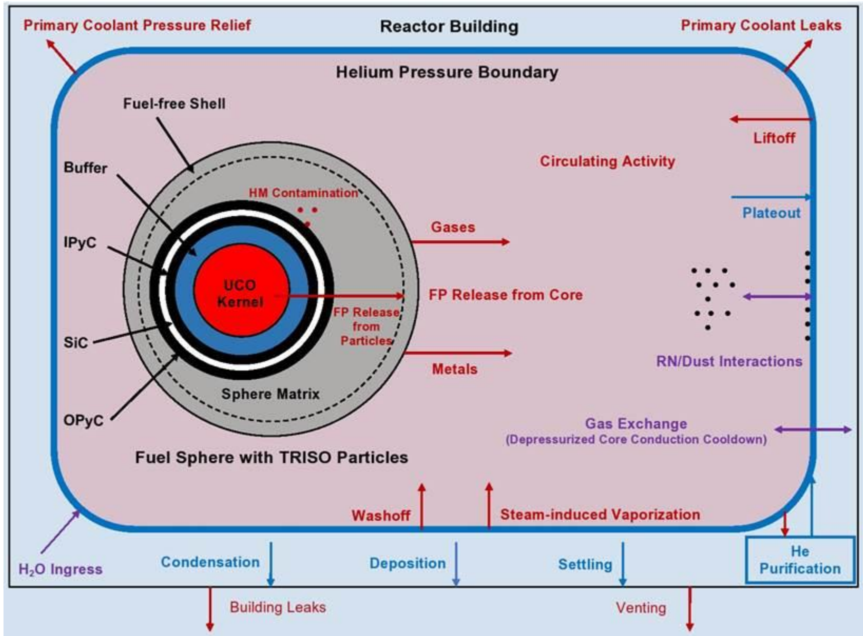

Figure 8. Pebble-bed HTGR radionuclide retention system.

The Southern Company (2019b) states that the defense-in-depth adequacy has three primary focuses: (1) risk-informed and performance-based (RIPB) DID adequacy, (2) capability DID adequacy, and (3) programmatic DID adequacy. The RIPB DID adequacy is primarily for developing and maintaining a basis for both supporting LBE selection as well as verifying that the entire plant conforms to cumulative risk targets. The plant-capability DID adequacy assessment involves both the identification of the layers of defense and the definition of the SSCs contributing to the layers of defense. The programmatic DID adequacy is for validating that proper treatment is considered for the design, operation, and maintenance of safety-significant SSCs. Figure 9 shows the overall process for incorporation and evaluation of DID that covers the aforementioned three main steps in DID adequacy. Tasks 1–8, 8–12, 13–17 in the figure are for RIPB DID adequacy, capability DID adequacy, and programmatic DID adequacy, respectively. The focus of this paper falls under the RIPB DID adequacy, and tasks 1–8 are as follows (for the complete DID adequacy discussion of the entire plant, refer to Southern Company [2019b]):

1. Establishing initial design capabilities, which include unique safety characteristics of the reactor design such as TRISO fuel.
2. Establishing F-C target based on regulatory objectives and quantitative health objectives, that are based on F-C target and cumulative risk metrics including the total frequency of exceeding a site boundary dose.
3. Defining SSC safety functions for PRA modeling such as prevention of radionuclide material release or control of decay heat removal.
4. Defining scope of the PRA that is usually dependent on the level of available design detail.
5. Performing PRA that uses initiating event groups to treat initiators that have common challenges to reactor and its systems.
6. Identifying and categorizing LBEs as Anticipated Operational Occurrences (AOO), DBEs, or Beyond DBEs (BDBE), which have different mean frequencies of exceedance values per year.
7. Evaluating licensing basis event risks versus F-C target.

8. Evaluating plant risks against cumulative risk targets that may include evaluating against average individual risk of early fatality within 1 mile of the EAB from all LBEs, average individual risk of latent cancer fatalities within 10 miles of EAB from all LBEs, and the total frequency of exceeding a site boundary dose of 100 mrem/plant-year from all LBEs.

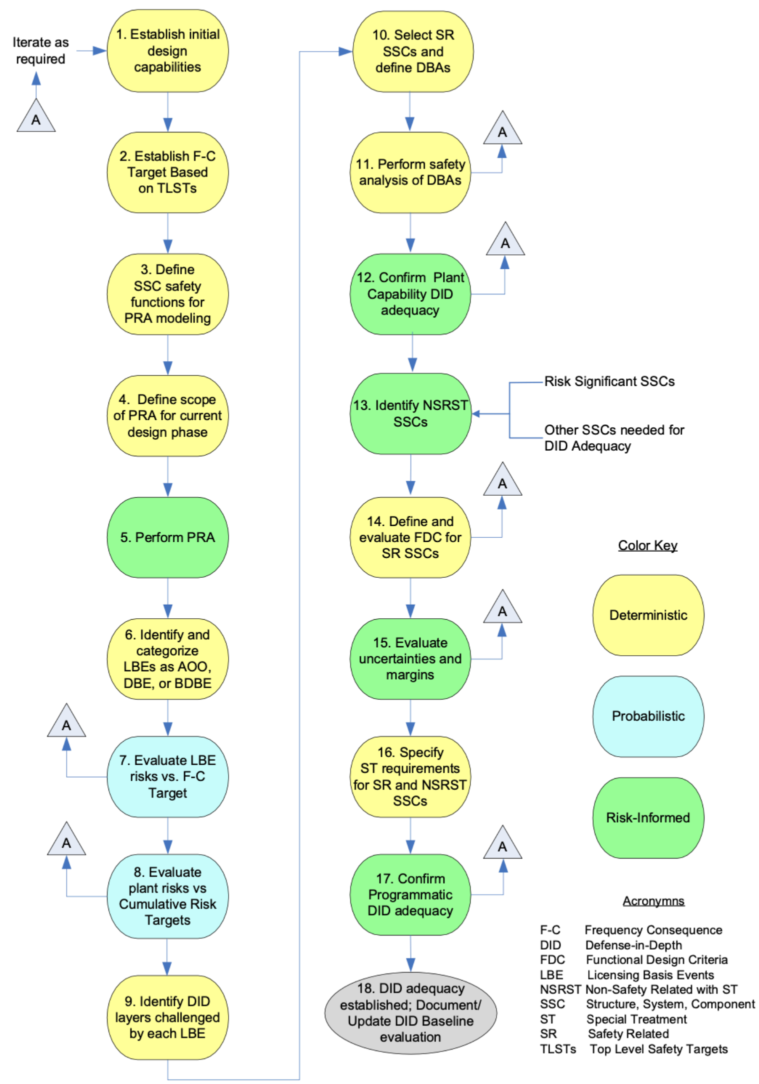

Figure 9. Proposed integrated process for incorporating and evaluating DID for risk-informed and performance-based design approach (Southern Company, 2019b).

The Southern Company (2019c) proposed technical requirements for licensing the Westinghouse eVinci™ microreactor. The microreactor is a high-temperature HP reactor, that is initially proposed to have three sets of barriers to prevent fission product release. The first barrier is the monolith encapsulation of the fuel in fuel channels. The second barrier is the surrounding monolith block. The third barrier is a canister containment subsystem that encases the entire core. Figure 10 shows the cutaway of the eVinci microreactor with its main components.

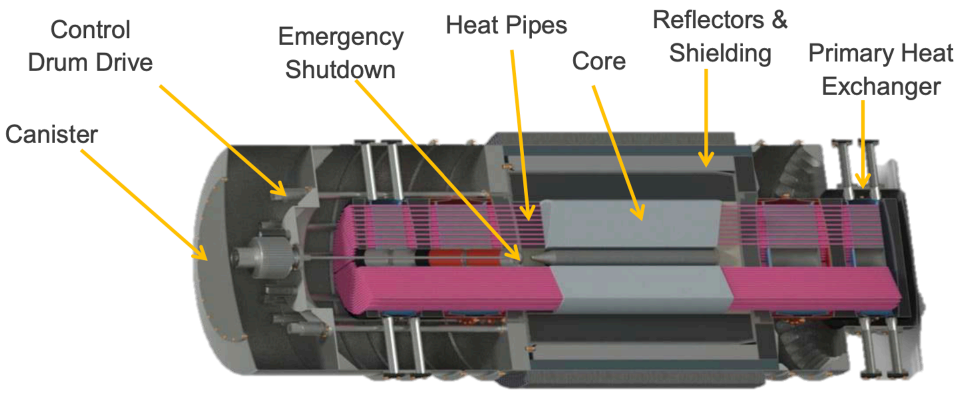

Figure 10. eVinci™ Microreactor cutaway.

A series of radiological consequence-based PRA calculations were prepared based on the eVinci™ reactor. The PRA defined the release path as from the monolith to canister (first barrier), canister to secure vault system (second barrier), and secure vault system to the environment (third barrier). The radiological consequences were based on five different release scenarios and temperature excursions (minimum, nominal, and maximum cases):

- Scenario (a) is all fuel channels release with a temperature excursion to peak of 950°C.
- Scenario (b) is all fuel channels release with a temperature excursion to peak of 850°C.
- Scenario (c) is all fuel channels release with a temperature excursion to peak of 750°C.
- Scenario (d) is a four-channel release with a temperature excursion to peak of 750°C.
- Scenario (e) is a gap release from four fuel channels.

Doses[a] were calculated by release scenario (a, b, c, d, e), number of barriers (i.e., 1, 2, or 3) and used a set leak rate of 0.001%/day. The highest doses were represented by scenarios where all fuel channels release, with the highest temperature excursions (i.e., 950°C), and release path with fewest barriers (i.e., 1). Calculations were made at power levels of 1 MWt (Table 2) and were scaled to 14 MWt (Table 3).

Table 2. Radiological consequences based on different release scenarios and 1 MWt power level.

FP Barriers	1 barrier			2 barriers			3 barriers		
Leak Rate	0.001%/day			0.001%/day			0.001%/day		
Section 4.3.1.2 Temperature Cases	Minimum	Nominal	Maximum	Minimum	Nominal	Maximum	Minimum	Nominal	Maximum
Release Scenario	30-day Dose at <1 m (rem TEDE)			30-day Dose at <1 m (rem TEDE)			30-day Dose at <1 m (rem TEDE)		
a	3.85E+00	4.82E+00	5.59E+00	5.00E-04	6.44E-04	7.25E-04	4.74E-08	6.15E-08	6.84E-08
b	6.25E-01	7.22E-01	1.14E+00	8.15E-05	9.59E-05	1.54E-04	7.73E-09	9.16E-09	1.48E-08
c	1.07E-01	1.15E-01	1.49E-01	1.41E-05	1.50E-05	2.00E-05	1.35E-09	1.42E-09	1.91E-09
d	1.43E-03	1.53E-03	1.99E-03	1.88E-07	1.99E-07	2.66E-07	1.80E-11	1.89E-11	2.55E-11
e	5.11E-04	5.11E-04	5.11E-04	6.65E-08	6.65E-08	6.65E-08	6.33E-12	6.33E-12	6.33E-12

Table 3. Radiological consequences based on different release scenarios and 14 MWt power level.

FP Barriers	1 barrier	2 barriers	3 barriers

[a] Based on 30-day Dose at <1 m, in units of roentgen equivalent man total effective dose equivalent (rem TEDE).

FP Barriers	1 barrier			2 barriers			3 barriers		
Leak Rate	0.001%/day			0.001%/day			0.001%/day		
Section 4.3.1.2 Temperature Cases	Minimum	Nominal	Maximum	Minimum	Nominal	Maximum	Minimum	Nominal	Maximum
Release Scenario	30-day Dose at <1 m (rem TEDE)			30-day Dose at <1 m (rem TEDE)			30-day Dose at <1 m (rem TEDE)		
a	5.39E+01	6.75E+01	7.83E+01	7.00E-03	9.01E-03	1.01E-02	6.63E-07	8.62E-07	9.58E-07
b	8.75E+00	1.01E+01	1.60E+01	1.14E-03	1.34E-03	2.15E-03	1.08E-07	1.28E-07	2.07E-07
c	1.50E+00	1.61E+00	2.09E+00	1.98E-04	2.09E-04	2.79E-04	1.89E-08	1.99E-08	2.68E-08
d	1.43E-03	1.53E-03	1.99E-03	1.88E-07	1.99E-07	2.66E-07	1.80E-11	1.89E-11	2.55E-11
e	5.11E-04	5.11E-04	5.11E-04	6.65E-08	6.65E-08	6.65E-08	6.33E-12	6.33E-12	6.33E-12

To illustrate this analysis, the consequence of removing the third barrier on the eVinci™ reactor is shown in Figure 11. If the canister containment system that performs the PRA safety function of containment, is not available, then the consequence is that (on average) the dose will not remain under the F-C target curve. In other words, removal of the boundary results in an unacceptable dose (dose case 4), given the frequency of these events (dose case 3). Reducing the frequency of the event could result in staying within acceptable limits.

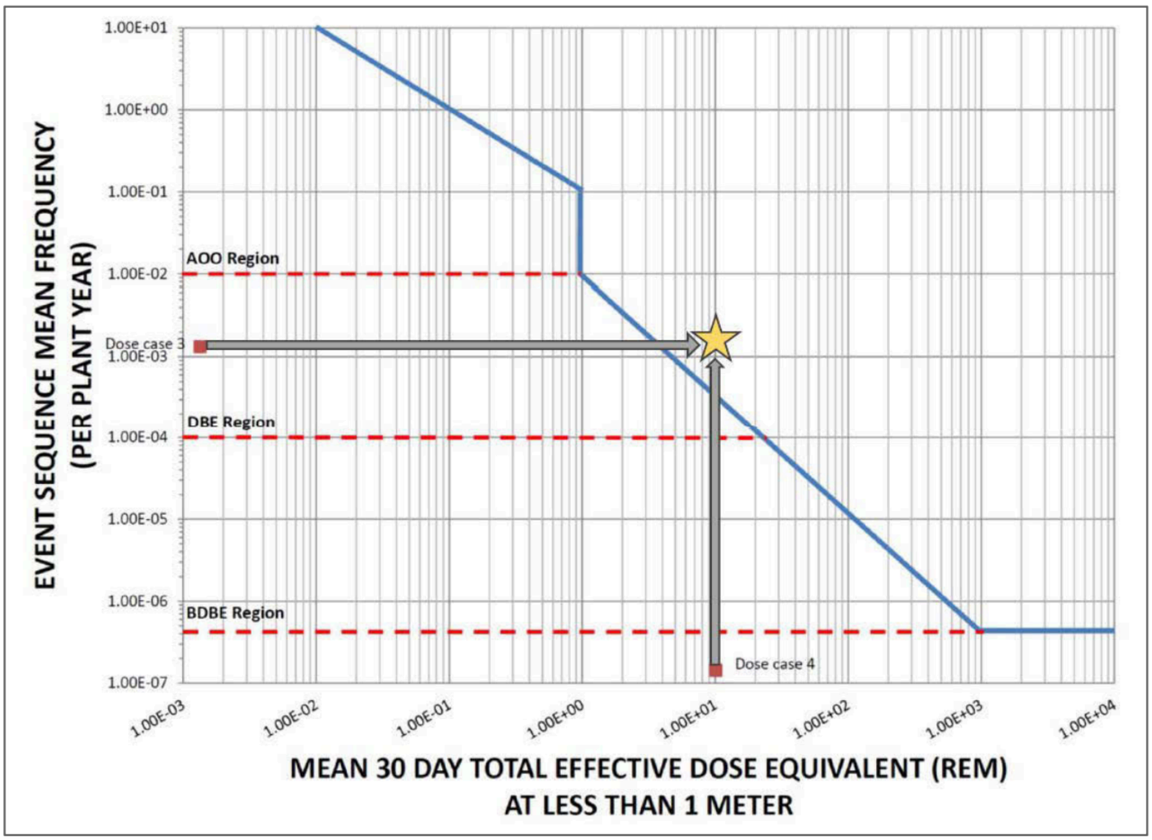

Figure 11. Comparison of different dose cases showing consequence without canister containment subsystem of eVinci™.

1.3 Economics of Microreactors

The Generation IV International Forum (GIF) developed the Advanced Nuclear Technology Cost Reduction strategies and Systematic Economic Review (ANTSER) framework for evaluating cost reduction opportunities for Gen IV nuclear concepts, based on functional containment approaches which are exemplified by the U.S. NRC ongoing development of the TI-RIPB regulatory scheme for non-LWR designs (Shropshire et al. 2021). The ANTSER framework was also used to evaluate modularity for nuclear energy applications at different scales. Modularity options for traditional nuclear energy deployment have been limited as a result of conventional LWR safety requirements, such as those related to high-pressure-retaining, heavy and robust containment structures. However, use of functional containment could enable less expensive and more flexible designs for microreactors (Kurt et al. 2022).

Related microreactor cost studies from Nuclear Energy Institute (NEI), INL, and others are also noted. Results from the initial ANTSER studies on functional containment and modularity as well as use of the framework may be used in the assessment of trade-offs between design concepts to achieve cost, safety, and performance goals. Given the recent development of microreactor designs, few bottom-up studies of microreactor costs are available.

1.3.1 Functional Containment

The NRC describes a "functional containment" approach as the full set of barriers designed to prevent any release of radioactive material into the environment. Hence, the functional containment approach can shift the nuclear plant design from satisfying rigid LWR-style prescriptive requirements toward considering multiple possible solutions in a TI-RIPB manner (Moe 2018).

Nuclear safety involves minimizing risks to plant workers, the broader public, and the environment based on detailed analyses of the probabilities and adverse impacts of possible scenarios. In the context of nuclear modeling and simulation, the probabilities of possible scenarios are referred to as frequencies (usually on the order of 10^{-3} to 10^{-7} per simulated reactor-year of operation) by the NRC, and the impacts are referred to as consequence. With this terminology, the risk inherent in each possible scenario can be calculated by multiplying the frequency by the consequence. Therefore, minimizing nuclear safety risks involves minimizing the frequency (probability) of possible scenarios, minimizing the consequence, or minimizing both frequency and consequence. Figure 12 illustrates the conceptual basis for nuclear safety requirements (Shropshire et al. 2021).

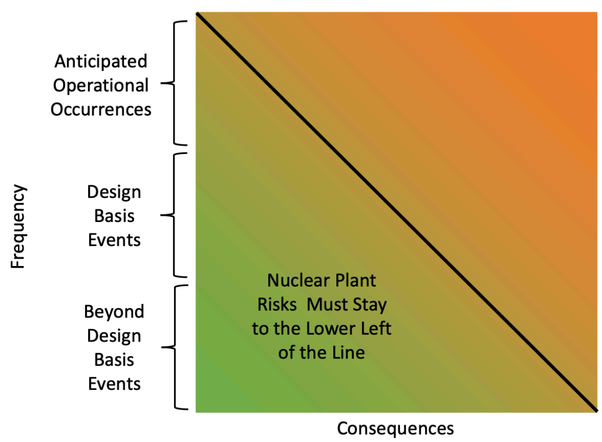

Figure 12. Potential increase (from green to orange) of reactor deployment cost based on risk-based design.

The TI-RIPB framework approach for advanced reactors enables use of a combination of different options in design, which can lead to different costs and overall associated risks. For example, a design could mitigate risks by use of seismic isolators for the reactor vessel and heat exchangers, embedment of the reactor building, and reducing the safety classification for the rest of the plant. Alternatively, a design could site the plant on the surface, use seismic isolators as base isolators and use robust modular shielding walls for the reactor building. Designs could be developed iteratively, which includes SSCs with different safety classifications, costs, and safety features. The selection of these options is highly dependent on the regulatory scheme and inherent safety features of the reactor design, such as use of TRISO fuel. The objective is to optimize each design to meet safety requirements at the least cost (GIF 2021).

1.3.2 Modularity-at-Scale

Modularity can include the incorporation of all major safety-significant systems – within one module, standardized modules, and factory-fabricated modules – the capacity to add modules to increase power output and the consolidation of components resulting in less on-site construction. Focusing on reactor modularity alone is insufficient to improve the cost competitiveness of nuclear energy technologies. Historically, modularity has been limited to the balance of plant for large-scale nuclear plants, such as steel-plate composite walls. These technologies have achieved limited success because of the need for extensive on-site capabilities. Modularity applications for small-, medium-, and micro scale plants are less well-known given their limited deployment. Modularity effects for microreactors could result in greater first-of-a-kind through nth-of-a-kind learning due to higher production quantities for the smaller plants to reach the same capacity as larger plants (GIF 2022).

To illustrate the concepts from the GIF study, Table 4 outlines the potential compatibility of reactor technologies with modular construction technologies applied to the balance of plant. LWRs need high robust containment structures as a result of their safety requirements. As shown in the red cells, modular precast construction is not compatible with large- and medium-sized LWRs. On the other hand, modular steel-plate composite (SC)-type construction is compatible with LWRs, although the data demonstrates considerable challenges during deployment. Modular precast construction is potentially compatible with GCR and SFR given the operational environment and containment at the fuel. Modular precast construction is a more mature technology compared to modular SC-type technologies. It is widely available among global suppliers and is less dependent upon site services, such as those that require high volumes of concrete or nuclear-grade welding (GIF 2022).

Table 4. Compatibility of different modular reactor technologies to modular balance of plant.

	Modular Precast Construction			Modular SC-type Construction		
	Large-size plants	Medium-size plants	Micro-reactors	Large-size plants	Medium-size plants	Micro reactors
LWR						
HTGR						
SFR/Thermal Micro reactor						

Legend: Red=not compatible, Green=compatible, Yellow=compatible, but may not be cost efficient

The GIF study concludes that the greatest potential for cost savings on advanced reactors could be achieved through design strategies that employ proven modularity concepts along with functional containment to create flexible designs. Further alignment is encouraged in the modularity concepts successfully deployed by the non-nuclear industry. The outcome of this strategic cost reduction activity is to expand information sharing within the GIF and among other stakeholders to accelerate progress toward the global deployment of cost-competitive nuclear plants (Kurt et al. 2022).

1.3.3 Additional Economic Studies

The NEI conducted a study (NEI 2019) on a reference 10-MWe microreactor plant based on proprietary data from several microreactor developers. This study notes that cost reductions are likely as more units are produced, and that microreactors are expected to follow learning rates similar to those in manufacturing industries, where learning rates of 15 to 20% are evidenced.

A bottom-up cost study (Abou-Jaoude et al. 2021) on microreactors employing the Generation IV code of account framework to incorporate the design features of a microreactor based on publicly available literature for a HP reactor. This study identified changes to some of the Gen IV accounts to better fit with the microreactor design. The capital costs of this representative microreactor were estimated by employing scaling algorithms to adapt elements and their associated costs. The levelized cost of electricity (LCOE) estimates were also estimated by using estimated O&M costs, fuel costs, and financing costs. The study found that over half of the contributions to the LCOE of this microreactor design stem from direct capital costs, as is consistent with studies on large nuclear power plants and SMRs. The second largest contributor to the microreactor LCOE is the initial fuel load.

Another study (Black et al. 2022) notes that the nuclear cost literature historically rests on economies of scale in power output, but SMRs and microreactors have shifted the focus toward economies of factory production and modularity to achieve cost reductions. This study further concludes that future markets where microreactors could operate competitively may rely less on economics and more on additional measures, such as reliability and resiliency, flexibility, mobility, etc.

2. MICROREACTOR TECHNOLOGIES

Current microreactor technologies under development in the U.S. include GCR, MSR, HP, and sodium fast reactors (SFR). There are no light-water microreactors included in this study due to a lack of current U.S. vendor designs. The general differences in microreactor technologies under development are provided in Table 5.

Table 5. Comparison of U.S. microreactor technologies and associated barrier approaches.

	GCR	MSR	HP	SFR
Capacity Range (MWe)	1–17	10–12	1–20	0.5–1.5
Fuels (HALEU, etc.)	TRISO	LEU, UF4	Metal, TRISO, Sodium	Metal
Coolant Systems	Helium, CO_2	Fluoride salt, FLiBe	FLiBe, Liquid Metal, Sodium	Sodium
Principal Barrier Systems[b]	TRISO fuel	Vessel and/or Containment	TRISO fuel (if used), or Containment	Vessel and/or Containment

2.1 Gas-Cooled Reactors

According to the International Atomic Energy Agency (IAEA n.d.) Advanced Reactors Information System (ARIS), many countries are developing GCR designs that use helium as a coolant due to their high fuel utilization rates and efficiencies owed to high-temperature operation. GCRs are being designed to burn TRISO fuel with enrichments up to 19.7% U235. They are cooled by gases including helium or carbon dioxide. These reactors could produce process heat for hydrogen production and low-temperature operations such as seawater desalination and district heating. U.S. microreactor developers proposing to use GCR designs include BWXT (BANR), General Atomics (GA Micro), HolosGen (HolosQuad), NuGen LLC (NuGen Engine), Radiant Nuclear (Kaleidos Battery), and X-Energy (Xe-Mobile), (Black et al. 2022).

2.2 Molten Salt Reactors

IAEA describes MSRs as a promising advanced reactor technology due to their operation at higher temperatures to improve performance, and low operating pressures which enhance the safety of the reactor. They may also generate less high-level waste resulting from solid fuel and potential to adapt to a variety of nuclear fuel cycles (such as Uranium-Plutonium and Thorium-Uranium cycles). MSR may be designed as nuclear waste “burners” or breeders. The high-temperature heat generated by MSRs may be used for electricity generation and for other high-temperature process heat applications. U.S. microreactor

[b] Barrier which serves to retain the highest quantity of radionuclides.

developers proposing to use MSR designs include Alpha Tech Research Corp. (ARC Nuclear Generator) and the Micro Nuclear, LLC (Micro Scale Nuclear Battery).

2.3 Heat Pipe Reactors

Compared to other microreactor designs, an HP reactor is a simplified reactor that omits the main pipeline, circulating pump, and auxiliary equipment. HP reactors include a monolithic core and highly efficient energy conversion system. The reactor is a fast spectrum, compact assembly of hexagonal fuel elements, each cooled by an axial molybdenum HP and loaded with fully enriched UC-ZrC or Mo-UO2. In addition to possible terrestrial uses, HP reactor designs are also being investigated for space power applications. U.S. Microreactor developers considering use of HP designs include Micro Nuclear, LLC (Micro Scale Nuclear Battery), NuScale Power (NuScale Microreactor) and Westinghouse (eVINCI^{TM}).

2.4 Sodium Fast Reactors

IAEA's ARIS lists fast reactors as using a fast neutron spectrum to increase the energy yield from natural uranium as compared to thermal (light-water) reactors. SFRs use UZr metal fuels, UO2, or advanced fuels. Fast reactors have potential to be used to breed nuclear fuel and be used as high-level waste burners. The sodium fast reactor is the most mature fast reactor design among lead, lead-bismuth, and gas-cooled fast reactors. The SFR has more than 400 reactor-years of experience acquired through the design, construction, operation, and decommissioning of experimental, prototype, demonstration, and commercial units operating in a number of countries, including the United States.

Oklo Power LLC submitted to the U.S. NRC a combined license application for review of the Oklo Aurora reactor based on Experimental Breeder Reactor-II and space reactor legacy. NRC denied the application, without prejudice, in January 2022. Subsequently Oklo has restarted licensing procedures. The 1.5 MWe reactor uses metallic fuel and sodium coolant, and heat pipes to transport heat from the reactor core to a power conversion system.

3. METHODOLOGY

This study involves a performance-based and risk-informed analysis design approach by introducing additional barriers to limit the dose of a microreactor system to remain under F-C target curves.

3.1 Performance-based and Risk-informed Design Considerations

The performance-based and risk-informed analysis design approach can be summarized as follows; however, the case studies presented here are simplified to communicate the approach rather than running and providing absolute numbers:

1. Identifying technology-specific safety features and licensing basis events.
2. Determining the frequency of occurrence and potential consequences of each event.
3. Evaluating the effectiveness of reactor safety measures in controlling the risks and the frequency of certain consequences.
4. Determining whether additional safety measures, such as additional barriers for radionuclide retention, are necessary to reduce the risk to acceptable levels.
5. Comparing the performance (see Sect. 3.3.1) and performance-based cost of different barrier designs and their risk control capabilities to determine which one is more appropriate.
6. Iterating on the design of additional barriers to balance the associated cost, risk, and performance of the microreactor system.

Although the study relies on common engineering analysis, risk management, and trade-off analysis, it is not easy to conduct a very detailed analysis on the topic. This is due to the limitations on available data related to commercial microreactor deployment, evolving regulatory practices, and site data on how additional barriers may perform in real life. Qualitative or semi-quantitative analysis can be performed for sensitivity analysis of different number of reactors and reactor outputs. The literature is reviewed and presented on the technology-specific reactor release rates and fractions, effects of performance of an additional structural enclosure, and related cost estimations for microreactors. These findings were used during the sensitivity analysis in the case studies.

3.1.1 Reliability of Passive Heat Removal Systems

The passive safety characteristics of non-LWRs were evaluated by MIT researchers (MIT 2018). They found that GCRs provide higher levels of inherent and passive safety than LWRs because of lower power density coupled with high heat capacity of graphite and passive heat removal from the core and reactor vessel. Passive shutdown from negative reactivity feedback in anticipated transients without scram and other transients has been demonstrated on existing smaller versions of GCRs. Researchers further noted that achieving negative reactivity feedback is less difficult for microreactors given the lower neutron leakage and positive reactivity void coefficient. Passive heat removal is also less difficult given the smaller decay heat load and lower surface-to-volume ratio of a microreactor compared to a large SFR.

Passive safety is also generally achieved through HP reactors and MSRs. Like HP reactors, MSRs may rely on a decay heat removal system that employs one or more intermediary fluids in a natural convection that can be subsequently cooled by ambient air. This system is commonly referred to as a Direct Reactor Auxiliary Cooling System (DRACS). Some designs may be cooled through the inherent conduction pathway from the core to the surrounding environment, commonly referred to as “conduction to ground.”

3.1.2 Reactivity Control

Reactivity control considerations could vary among advanced reactors. GCRs could benefit from lower costs for reactivity control compared to LWRs due to no runaway meltdown risk. (INL 2021)

3.1.3 Radioactive Material Containment

Radioactive material release into the environment is prevented through a set of barriers. Current LWR plants have large, heavy, and costly pressure-retaining concrete containment structures to prevent the release of fission products in the case of a severe accident. The functional containment approach provides an opportunity for innovative alternatives to the traditional containment structure while maintaining (or ideally improving upon) safety performance. Such a gain in design flexibility and cost reduction is enabled by the inherent advantages of advanced designs. The approach also allows for a combination of innovative alternatives to prevent the release of radioactive materials, protect against external hazards, and produce site-independent designs such as seismic isolators, underground embedment, accident tolerant fuels and passive safety systems (Shropshire et al. 2021).

3.2 Economic Considerations

While economic considerations are factored into the analysis, designers often avoid altering fundamental design choices (e.g., coolant type, neutron spectrum, fuel type) based on these aspects. This is especially the case for traditional plant designs, fuel cycles, and other major systems based on previous generations, leaving little flexibility for significant changes. However, for a non-LWR-based microreactor designed using a functional containment approach, opportunities are available to use advanced fuels, coolants, and reactor vessels to achieve safety requirements while producing an economic design.

3.2.1 Fuel Costs

According to the DOE Systems Analysis and Integration (SA&I) Campaign’s research, metal fuel fabrication costs range \$800/kgU (below 10% enriched) to \$6000/kgU (>10% and <20% enriched). The enrichment percentage of high-assay low-enriched uranium (HALEU) drives the requirement for ore (yellowcake), enrichment (SWUs), and conversion on a per-kilogram basis. The use of less fuel per unit of energy offsets the per kgU cost increase (DOE 2021).

The TRISO fuel manufacturing process is much more complex than for metal fuel and involves far more steps than the casting process for contact handled U-metal fuel. Quality assurance requirements are also much more stringent for TRISO particles. According to the DOE report (2021), the TRISO-particle fuel will be more expensive to fabricate on a per-kilogram of uranium basis, but that the reactor will use far less fuel (uranium) on an annualized basis than low-enriched uranium (LEU) fuel ($400/kgU). The nominal cost estimate for GCR TRISO fuel is $10,000/kgU.

No references were found on cost scaling for TRISO fuel. Because batch sizes are limited by criticality concerns, any capacity additions to an already-existing production scale facility (none exists now) will be accomplished by adding new process lines and the use of multiple shifts. The size of an optimal automated TRISO particle fabrication line will be determined by the market, which hopefully will include many reactor types and vendors. Compared to LWR fuel, reactors using TRISO and other advanced ceramic fuels have the advantages of longer in-core residence times, higher burnup, use of higher temperatures for increased thermodynamic efficiency of the reactor, and inherent safety due to the much higher melting point and lack of possible cladding fuel chemical reactions.

3.2.2 Coolant System Costs

Microreactor coolant costs make up a higher share of reactor costs, but the costs may be offset by higher reactor thermal efficiencies. According to an INL study (Abdalla Abou-Jaoude 2021) the HP reactor coolant system operates much differently and is a larger proportionate cost contributor to LCOE than for GCR and MSR designs. They found that for a hypothetical HP reactor, 74% of the total LCOE is made up by the initial fuel load, the building, the interest accrued, the reactor coolant system, the reactor control system, instrumentation and controls, and decommissioning. Advancements in HP technology to improve heat removal capacity could reduce these costs. For example, a design with 500 HPs at a unit price of $5,000/pipe would result in a $100/MWh drop in LCOE relative to a concept with 1,000 heat pipes at $10,000/pipe (Abdalla Abou-Jaoude 2021).

Unit prices for heat pipes will likely strongly depend on the associated manufacturing learning rates. For example, the previously mentioned price of $5,000/pipe could be reached after ~500 units with a first-of-a-kind cost of $10,000/pipe, with an initial learning rate of 5%, increasing to 10% after 70 units. The manufacturer will be presented with different opportunities to either reduce first-of-a-kind prices, improve learning efficiencies per unit, or increase the heat pipe capacity to reduce the total number of heat pipes needed per reactor. This could include design standardization, robust supply chains, advanced (additive) manufacturing, novel materials, etc. (EPRI 2018).

3.2.3 Reactor Building Costs

Microreactors are expected to minimize on-site building structures typically associated with nuclear reactors (e.g., turbine building, auxiliary building). Some microreactor concepts (e.g., Oklo) envision a single building to house the reactor, power conversion, operating room, and security facility. Others (e.g., eVinci™ and HolosGen) plan to use standard ISO containers in which the reactor modules are transported and house the reactor. The cost of the building structure is a function of the dimensional size (e.g., surface area, number of floors) and robustness of the structure (e.g., thickness, confinement, embedment), and utility requirements (e.g., connection costs, underground distance to utilities), as illustrated in Figure 13 (Abdalla Abou-Jaoude 2021).

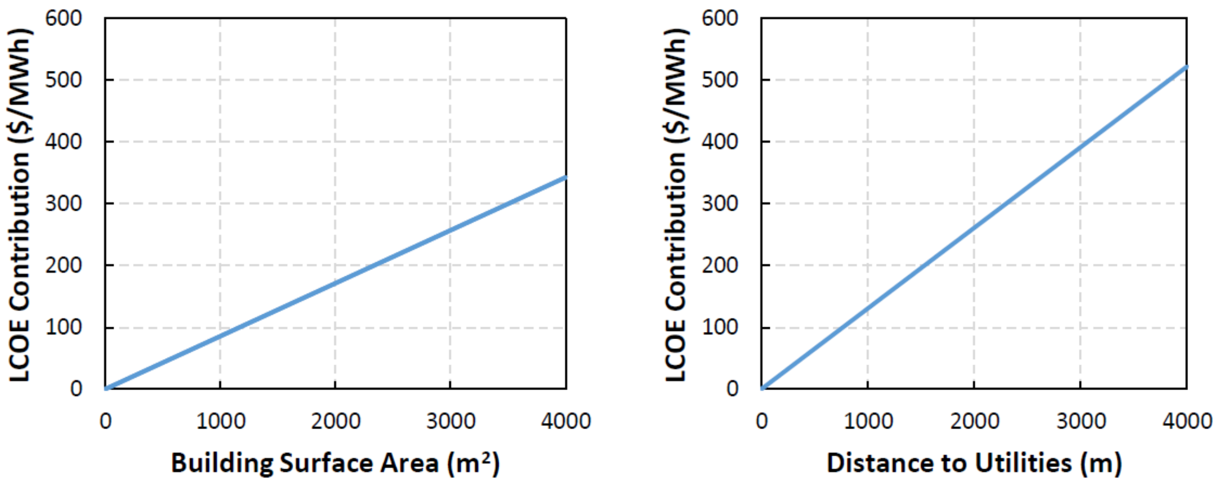

Figure 13. Contribution of the reactor building surface area and underground distance to utilities on the overall LCOE (Abdalla Abou-Jaoude 2021).

3.3 Approach for Evaluating Trade-offs Between Microreactor System Designs, Fuels and Reactor Module Sizes

The trade-off between cost, performance, and risk is a key decision-making factor in most of the industries. These industries include aircraft, medical, transportation, and construction industries. As an example, in the aircraft industry, the designers understand that the crew, customers, and the business are at increased risk if the aircraft performance starts to degrade under certain conditions or over time. So, designers of aircrafts may need to use relatively expensive materials or technologies to improve performance. However, they need to balance the cost, risk, and performance at a certain point that the product itself is desirable, reliable, and sustainable. Figure 14 represents such a point, where the desired or acceptable product bounded by unacceptable risks, performance, and costs. Similarly in the construction industry, the deployment of buildings is adjusted to balance the cost and performance based on the importance of the building and risk associated with degraded performance. Nuclear energy deployment, especially microreactor deployment, is also no exception in such discussions of balancing cost, performance, and risk.

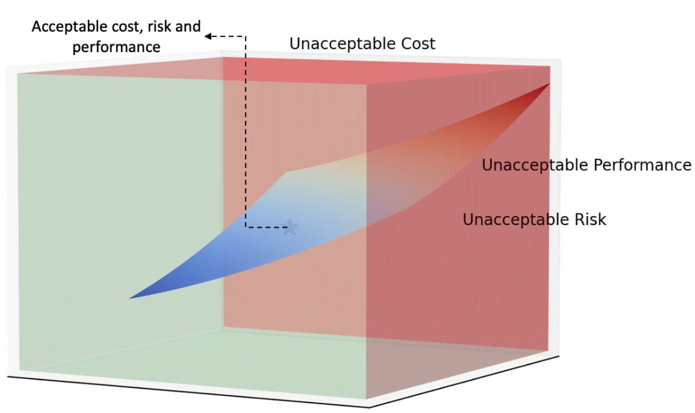

Figure 14. Schematic representation of design space with associated cost, risk and performance.

The overall cost of the microreactor systems depend on several factors including the size, complexity, type, mission, and location of the reactors. Microreactors are also unique in the sense that they are small, mobile, and expected to be low maintenance. However, there is also risk associated with them. Under some circumstances, the microreactors may need additional barriers to retain the release of radionuclides and reduce the associated risk. The rest of the study discusses introducing an additional barrier in the form of structural enclosure to collocated microreactors. The discussion is on how to balance between the performance and cost of the additional barrier and how it potentially supports in reducing the risk. The cases studies include different thermal outputs to understand the benefits or trade-offs that arise from increasing the power levels under such circumstances.

3.3.1 Performance of the Structure

The effects of structural performance are discussed based on the basic principles of performance-based design. Performance-based design focuses on achieving specific performance targets for the structures, but estimations on how to achieve these targets are related to many factors, from site conditions to structural materials to the frequency of events that they are investigated under. Sometimes, these target goals include being fully operational, or focus on the life safety of occupants, or prevent collapse of a structure after a major event such as earthquake. The overall goal is to achieve durable, safe, and cost-efficient structures. Detailed discussion and analysis based on performance-based design is beyond the scope of this study.

The American Society of Civil Engineers (ASCE) standard, ASCE-43, is developed to provide requirements that ensure the reliability of nuclear facilities through the design and assessment of new or existing nuclear SSCs (ASCE 2022). ASCE-43 discusses how performance goals, in terms of probability of failure, are achieved while retaining the desired functionalities of nuclear facilities. The intent is to achieve specific performance goals for certain limit states. Four different limit states are considered: limit state (LS) D (LS-D), LS-C, LS-B, and LS-C. The expected damage for LS-D is negligible, which is essentially elastic behavior. LS-C is expected to have minimal damage, with a slight deviation from elastic behavior that causes limited permanent deformation. LS-B is generally a reparable damage state with moderate permanent deformations. LS-A is the worst limit state that ranges from significant damage to the structure to the structure being pushed to the limit short of collapse. Discussions such as detailed seismic analysis, soil-structure interaction, or consequences of liquefaction of soil are beyond the scope of this study. This work adopts the performance-based discussions of ASCE-43 but oversimplifies them within the scope of this study.

Figure 15 shows the capacity-deformation curve of a typical structural component. The shape of the curve will vary depending on the type of the element and the material, and represents the different stages of how the damage propagates. The elastic limit lasts until all the structural systems can recover back to their original positions after the causes of the deformation, such as earthquake loads, are removed. This region aligns with the LS-D limit state described in the text above. The permanent deformations come after the elastic limit region. The severity of the deformation is related to how irreparable they are, such as with large cracks on concrete elements, related to the extent of loading. The increased damage states can also be interpreted as a loss of functionality of the structure over time. The limit states of LS-C, LS-B, and LS-A are described above. This study assumes a similar progression of loss of functionality based on the limit states and associated damage states.

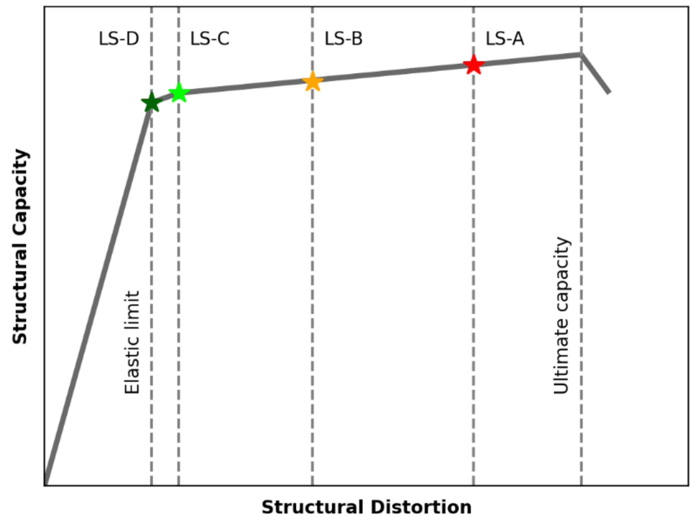

Figure 15. Typical capacity-deformation curve and limit states.

Figure 16 shows a representation of damage states associated with different limit states. This study considers the progression of concrete cracking geometry, as it can be directly related to the retention capacity of such concrete structural enclosures (Bejaoui et al. 2007).

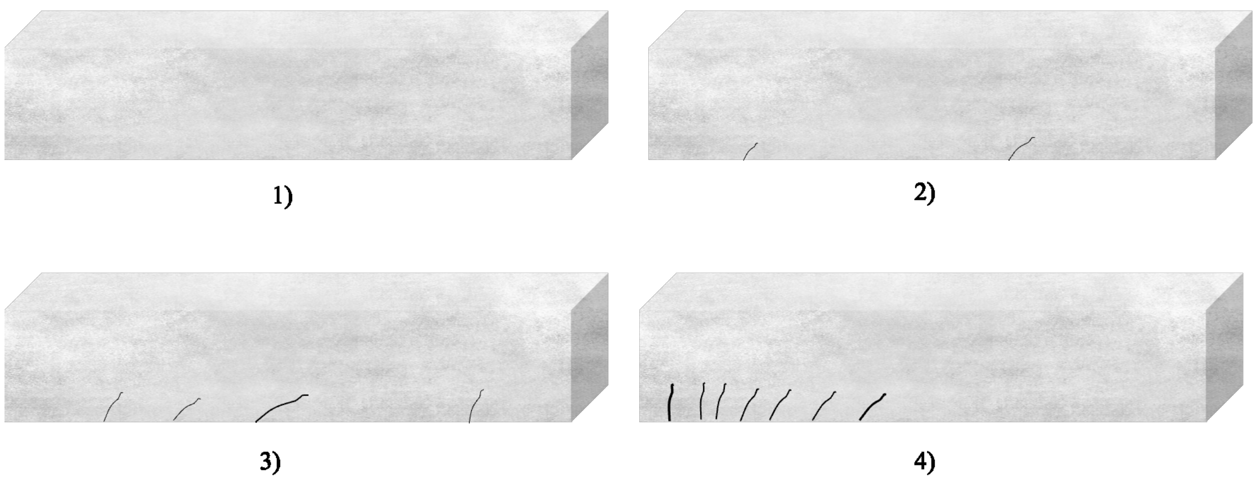

Figure 16. Representative progression of damage states, such as crack geometry, at different limit states: (1) LS-D, (2) LS-C, (3) LS-B, and (4) LS-A.

3.3.2 Cost and Layout of the Structure

Calculating the cost of even a simple nuclear-grade structure is a complex process. There are many factors and regulations that may affect the final cost. Size of the structure is one of the most important factors, as it has direct implications on the cost through materials used, site work needed, on-site work, and manufacturing process. This study assumes a simple structure in the shape of a rectangular prism as an alternative to the standard container-express (CONEX) shipping boxes proposed by the industry. In this study, the CONEX box-type structure is assumed to provide some relief from climatic conditions but has no effect on radionuclide retention. Thus, a nuclear-grade concrete structure is implemented as an additional radionuclide retention barrier when needed.

Alternative designs of the enclosing structure may result in different total cost. A more robust and complex structure costs more than a same-size structure with a less complicated structural system. This is represented by the effect of structural complexity with the factors shown in Table 6. An elastic structural system is assumed as the baseline and has an impact factor of 1.00 on the cost. A structural system with behaviors in the range of LS-C is assumed to have a factor of 0.95. The system response after a major event, such as earthquakes or floods, is close to elastic limit, but has some inelastic deformations that do not necessarily affect the integrity of the structure. It is assumed that the structural system with LS-C can be easily repaired and has minor cracking in its geometry. An LS-B type of system may show some inelastic geometry after a major event where the structure is not immediately reparable and may have partial impact on radionuclide retention. On the other hand, a structural system that has deformed to LS-D levels is assumed to fail. Failure is defined as losing the capability of radionuclide retention. The LS-D case is similar to a CONEX box-type enclosure for radionuclide retention.

The performance-based design of structures is a highly specialized area of expertise. Detailed analysis of the structural geometry and materials, site conditions, and potential hazards is needed to assess how the structure will perform. This study assumes a simplified discussion on performance of the structures based on the limit states discussed above. Based on the functionality of the structure, such as radionuclide retention or staying intact after major hazards, and what performance level designers want, will affect the ultimate cost of the structural barrier. Reasonably, the more robust the system and the better its performance, the more costly the structure. As an example, a designer may increase the wall thicknesses to have better resilience against external hazards to obtain better performance, or they may prefer using a seismic isolator to reduce risk, but these changes result in increased capital cost.

Cost of the enclosure structures will highly depend on the site properties. Although no data are available for microreactor structural barriers and associated costs, some studies provide insights on how the cost of the structural system may change depending on the site conditions. Based on the design level, which may also be translated to performance level, the cost of the structural enclosure may change. Figure 17 shows the relation between cost and design level for non-nuclear structures at different sites around the U.S. (Ferritto 1984). Though the cost may change based on the seismicity of the site, the trend is similar. However, it can be assumed that the cost with reasonable performance levels may change within 25% of each other. This study does not consider specific sites or provide exact costs but rather describes relative delta costs as compared to a baseline. As discussed earlier, the design and associated cost will depend on numerous factors that are outside of the scope of this study.

All the analytical, design, and site condition complexities and associated increased costs for the structural system are summed under a structural complexity parameter in this study. Table 6 shows assumed values of the structural complexity parameter. The range of values is between 0.75 and 1.00. The value of 1.00 correlates to the structural barriers remaining elastic (i.e., no expected damage) which makes such structures the baseline cost in comparisons, and relatively the most expensive. If the design is relaxed, such as thinner wall sections, to reduce the costs, a value of 0.75 for the structural complexity is assumed. These ranges and values may change based on the detailed analysis, design, materials, and site conditions. However, this study assumes that there is a performance threshold expectation for nuclear structures, even though the design is being relaxed compared to an elastic state. Thus, a lower boundary of 25% cost reduction is used, corresponding to a more relaxed design.

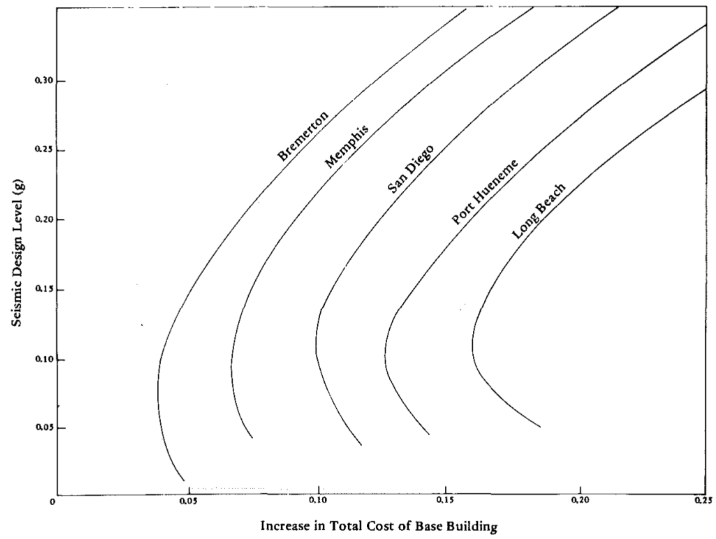

Figure 17. Increase in cost for a typical non-nuclear structure at different sites based on their seismic design level (from Ferritto 1984).

Table 6. Effect of structural complexity on the cost.

	LS-D	LS-C	LS-B	LS-A
Structural complexity	1.00	0.95	0.85	0.75

The structural system geometry is assumed as a rectangular prism. Due to the unique missions of microreactors, the vendors are leaning toward the ability of the reactor to be mobile (i.e., moved from one site to another). The discussions tend to include packing microreactors inside standardized CONEX boxes. This study assumes the dimensions of the microreactors to be equivalent to the dimensions of a 40-ft CONEX box. The length, width and height of the reactor are assumed as 40 ft × 8 ft × 8.5 ft, respectively. Below are the equations for calculating the dimensions of the structural enclosure system. It is assumed that the structure has planar dimensions of a reactor's length (l_r) and width (w_r). Additional planar space equal to the length and width of the reactor is added as represented in Figure 18. The reactor roof clearance is assumed to be 2-ft above the reactor height. The cost per unit volume (C_v) includes the engineering design, material cost manufacturing, site preparation, project management, and other associated activities.

t_s : thickness of the structure
l_s : length of the structure
w_s : width of the structure
h_s : height of the structure
C_v: : cost per unit volume
C_T : total cost of the structure systemN_r : number of reactors

There has not been a microreactor deployed in real life, but some studies estimate the cost of concrete structures for potential microreactors. When the historical cost data is scaled to microreactor sizes, Hoffman et al. estimated (2020) that a concrete structure cost will be around \$23/ft^3. This study assumes \$90/ft^3 to deploy a concrete structural enclosure around a microreactor, which includes design analysis and engineering, increased cost of materials since the estimations, additional on-site work, manufacturing, and other related activities. Table 7 shows estimations of deploying concrete structural enclosures based on their expected performance. Total costs are calculated per foot-thickness of wall. As expected, the cost of the structural system increases with greater structural complexity (i.e., increased robustness). Figure 18 shows a schematic view of the layout of the structural enclosure.

Table 7. Generic cost comparison of structural enclosures based on their expected performances and complexities.

	l_r (ft)	w_r (ft)	h_r (ft)	C_v	Structural Complexity	C_T (\$/ft wall thickness)
LS-D	40	8	8.5	0.05	1	1,500,000
LS-C	40	8	8.5	0.05	0.95	1,400,000
LS-B	40	8	8.5	0.05	0.85	1,250,000
LS-A	40	8	8.5	0.05	0.75	1,110,000

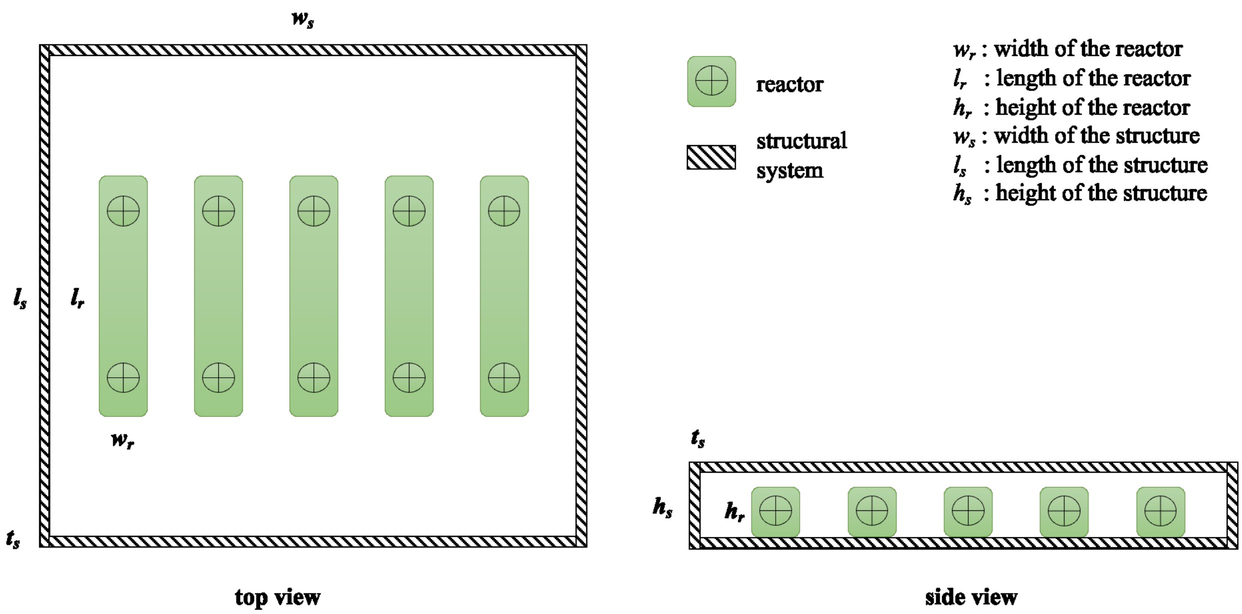

Figure 18. Schematic view of layout of the structural enclosure.

3.3.3 Simplification of Consequences

The F-C curve based on the LMP has three different regions: anticipated operational occurrence, design-basis events, and beyond-design-basis events. These regions are bounded by three straight lines, which put boundaries on the consequences of dose cases of different event sequences. In this study, the boundary in the F-C curve is simplified with a straight line. Two hypothetical event sequences were selected that represent dose case 1 and dose case 2. The event with dose case 1 is a high frequency and lower consequence dose case, whereas dose case 2 is a low frequency and higher consequence. The assumed containment functionality of the reactor is presented in dose case 1, whereas containment functionality is lost in the event of dose case 2. This can be due to fuel cracking or a damaged physical reactor containment enclosure. We assume that the consequence of dose case 1 will be equal to the dose in case 2 under the circumstances where the containment functionality is lost. Such a condition may or may not challenge the consequence to remain under the F-C target curve. Under the condition of the consequence not remaining under the target curve, an additional containment barrier may be necessary, and this additional barrier is represented as the concrete structural enclosure discussed above. Figure 19 represents this phenomenon, where an additional barrier is not present, and the consequence is challenged to remain under the FC target curve.

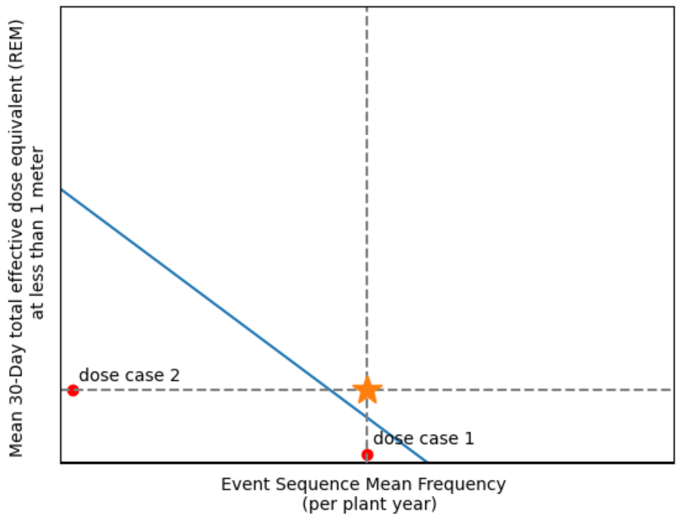

Figure 19. Representation of the consequences of dose cases when an additional barrier is not present (straight blue line is the F-C target).

4. ANALYSIS AND FINDINGS BY MICROREACTOR TECHNOLOGY

The goal of this effort is to evaluate different barriers for key microreactor types (GCR, MSR, HP) for potential economic and FP retention trade-offs. It is recognized that these barriers and buildings will have many other functions beyond FP retention. These other functions will play a strong role in determining their design attributes and parameters. However, if there are any features, such as filtration systems, that primarily serve a radionuclide retention function, some optimization may be possible using mechanistic source term (MST) analysis and functional containment.

Generally, the functional containment and economic evaluation approach will consist of the following steps:

1. Review technology background material and identify radionuclide inventories, barriers and their performance values, economic, and other information important to functional containment economic evaluations.
2. Set a reference radionuclide inventory for each reactor technology, for a specific power level.
3. Set barrier performance, radionuclide release fractions.
4. Evaluate scenarios with different barrier release fractions and economic costs.

The initial findings from this project can help to better focus the evaluation approach for future analysis.

4.1 Gas-Cooled Reactor Findings

For a 600 MWt prismatic HTGR (generalized in this study as a GCR), MST calculations were performed and documented as part of the next-generation nuclear plant (NGNP) project (INL 2012). Initial core FP inventories are listed in Table 8 for reference, with a simple scaling to 1 MWt for a crosstechnology comparison to be performed later.

Table 8. Initial core fission product inventories, in curies, adapted from NGNP (INL 2012).

Key Radionuclide	Reference 600 MWt	Scaled to 1 MWt
Xe-133	3.63E+07	6.05E+04
Kr-85	1.90E+05	3.17E+02
Kr-88	1.85E+07	3.08E+04
I-131	2.00E+07	3.33E+04
I-133	3.60E+07	6.00E+04
Te-132	2.71E+07	4.52E+04
Cs-137	1.69E+06	2.82E+03
Cs-134	1.90E+06	3.17E+03
Sr-90	1.69E+06	2.82E+03
Ag-110m	2.81E+04	4.68E+01
Ag-111	2.96E+06	4.93E+03
Sb-125	2.35E+05	3.92E+02
Ru-103	3.61E+07	6.02E+04
Ce-144	2.33E+07	3.88E+04
La-140	3.27E+07	5.45E+04
Pu-239	4.66E+03	7.77E+00

GCRs generally rely on TRISO-based fuel which contains several different barriers within the principal fuel unit. The fuel then acts as a strong barrier to radionuclide release, relieving other barriers, such as large containment structures, from having to perform this function (EPRI 2019). However, the helium pressure boundary (HPB) and reactor building (RB) structures still act to contain some radionuclides in a worst-case accident.

Barrier performance can either be assessed by its release fraction, which may vary by radionuclide, or by its attenuation factor. The attenuation factor is simply the inverse of the release fraction. Ideally, an MST analysis with design-specific features would be used to estimate barrier release fractions. However, for the purpose of presenting the approach, generic estimates can be assumed. Then, parametric studies can be performed to demonstrate an approach to assessing potential economic benefits while meeting all applicable safety criteria. Figure 20 shows some of the key GCR radionuclide barriers and the pathway for release.

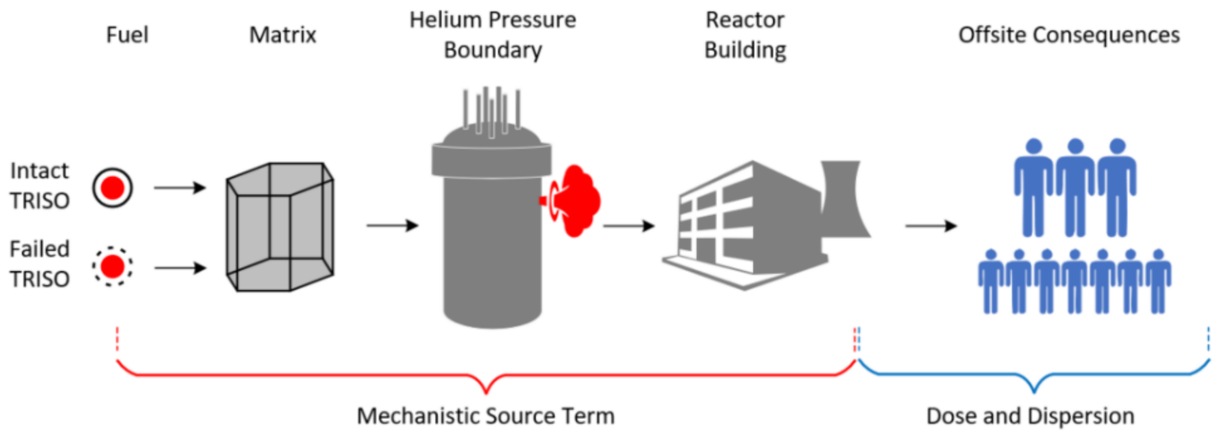

Figure 20. GCR key barriers and a pathway for radionuclide release.

From these NGNP references (INL 2012, EPRI 2019, Naido and Kleming 2009), barrier release fractions by FP class are assumed and makeup the reference condition as shown in Table 9.

Table 9. Reference barrier release fractions for a generic, prismatic HTGR, worst-case HPB break accident, adapted from NGNP References (INL 2012).

TRISO Fraction	Fission Product Class	From TRISO into Matrix	From Matrix into Helium	From HPB into RB	From RB into Environment	Product (Total Fraction of Inventory)
Failed Fraction = 2.3E-5	Noble Gases	0.2	1.0	0.5	1.0	2.30E-6
	I, Br, Se, Te	0.2	1.0	0.5	0.5	1.15E-6
	Cs, Rb	1.0	0.33	0.33	0.5	1.25E-6
	Sr, Ba, Eu	1.0	3.3E-2	0.33	0.5	1.25E-7
	Ag, Pd	1.0	1.0	0.33	0.5	3.80E-6
	Sb	1.0	3.3E-2	0.33	0.5	1.25E-7
	Mo, Ru, Rh, Tc	0.02	0.33	0.33	0.5	2.50E-8
	La, Ce	0.02	3.3E-2	0.33	0.5	2.50E-9
	Pu, actinides	2.0E-3	3.3E-3	0.33	0.5	3.76E-11
Intact Fraction = 0.999977	Ag, Pd	0.01	1.0	0.33	0.5	1.65E-3
	All other Fission Product Classes	0.0	—	—	—	0.0

From Table 9 the last column can then be multiplied by the radionuclide inventories presented in Table 8 to estimate a conservative, worst-case accidental release to the environment. To arrive at an offsite dose and public health consequences, radionuclide dispersion calculations should be performed, with site-specific features taken into account. A generic site, methodology (Fair and Huning 2021), and dose cacluation tool (LLNL 2010) can then be used for the purposes of evaluting the combined economic and safety benefits of varying release rates for each barrier.

In terms of estimating the dose from a worst-case accident (i.e., dose using release fractions presented in Table 9), a conservative set of dispersion assumptions are followed:

1. Ground release (e.g., initial source height = 0 m away from the ground).

2. Wind stability class “F” (e.g., 1 m/s).
3. No ground shine or resuspension.
4. Dose conversion factors (DCFs) based on EPA FGR-13 (ICRP-60, 1991).
5. Standard/rural terrain.
6. Breathing rate of 4.414E-04 m^3/s.

Using these parameters, the radionuclide release fractions, and inventory for a 1 MWt GCR, the total effective dose (TED) as a function of distance from the release for three different cases are shown in Figure 21.

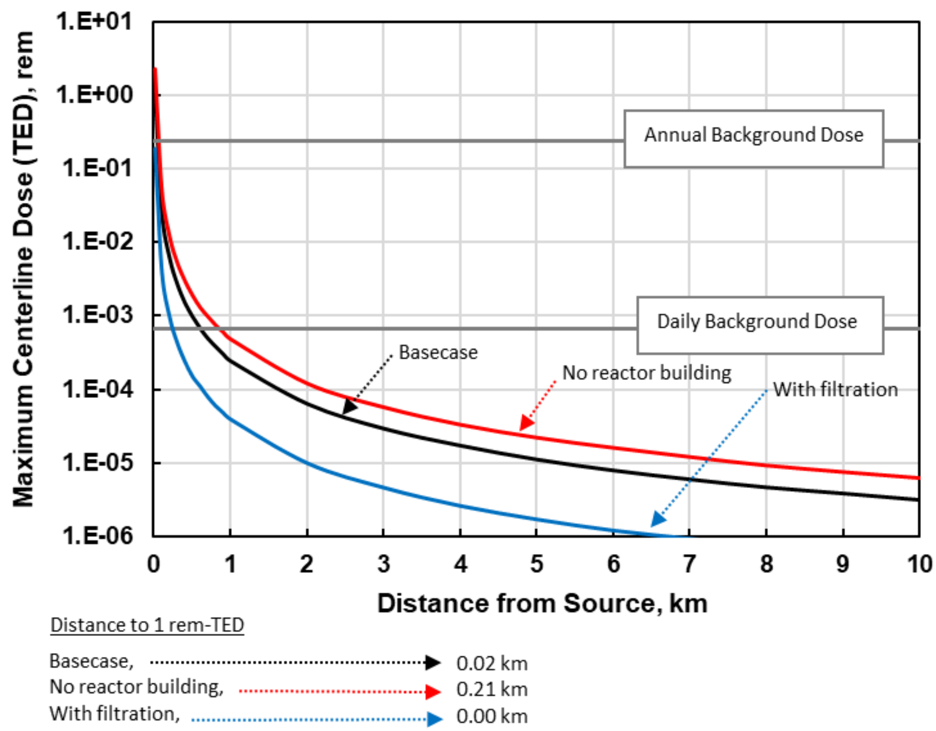

Figure 21. GCR centerline dose as a function of distance from source.

The basecase assumes the RB release fractions shown below in Table 9. The “no-reactor building case” assumes all radionuclide release fractions from the RB are 1.0. The “with filtration” case assumes all ideal gases are released, but 95% of all other radionuclides, except for iodine, are retained. Iodine generally requires special filters and active cooling to prevent volitilization. For all cases, including the case that neglects any RB retention, the distance to 1 rem-TED is less than 210m. Doses quickly approach and fall below the daily background level around 1 km under the worst, no-RB case.

The 1 rem-TED is a common metric as the Environmental Protection Agency’s protective action guidelines (PAG) recommend sheltering-in-place or evacuation of the public if the projected dose over four days is greater than 1 rem (EPA 2017). Given these results, it is unlikely that a 1 MWt GCR would need these PAG-required emergency planning actions. This opens up some opportunity for higher power levels or optimization of barriers that would reduce overall cost while meeting all required safety limits.

4.2 Molten Salt Reactor Findings

Liquid-fueled MSRs have substantially different source terms and release characteristics than other reactor design types. As with most designs, a break in the primary vessel, spent fuel, or waste stores would be necessary to achieve any significant offsite release. However, MSR release data is more limited than for TRISO and conventional LWR fuels. MSR release phenomena are depicted in Figure 22.

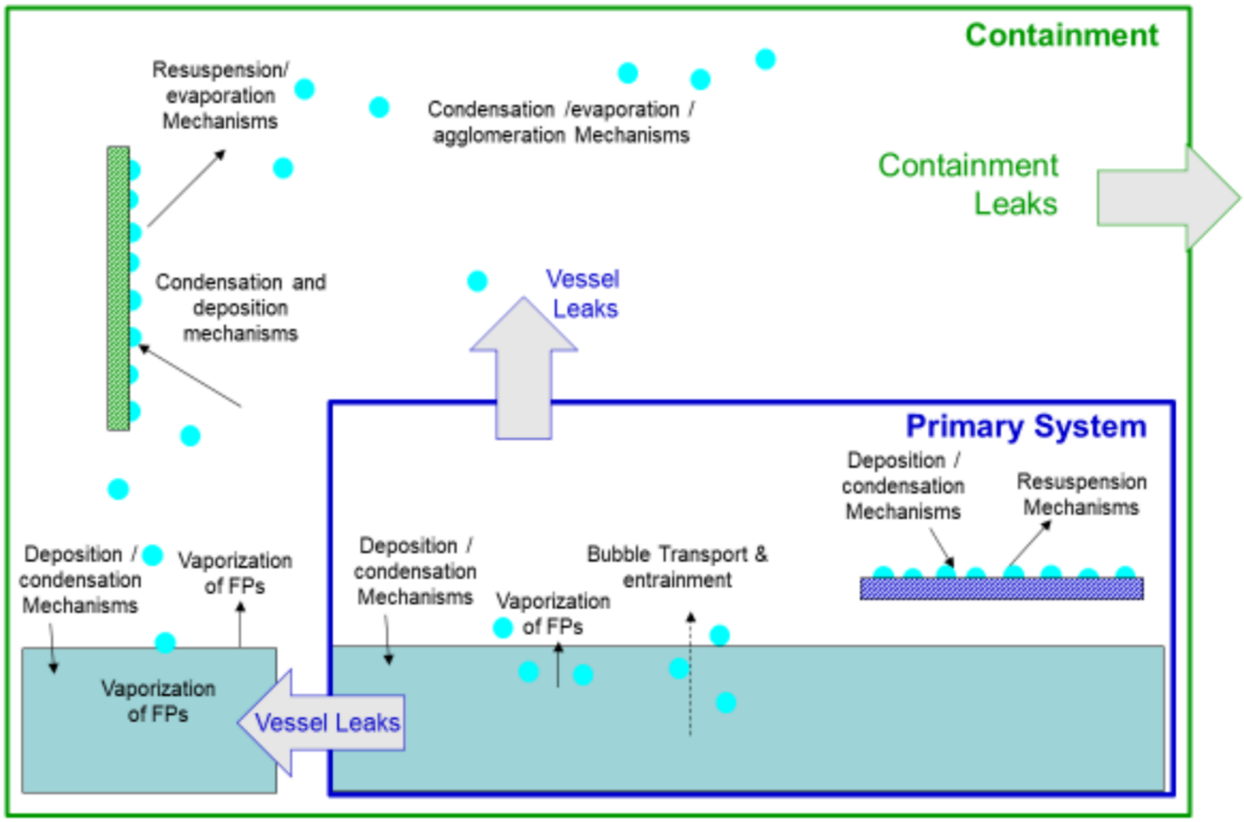

Figure 22. Schematic diagram of radionuclide transport and release paths for liquid-fueled MSRs (NRC 2019).

For the MSR Experiment, conservative release rates were assumed between the barriers for its documented maximum credible accident (Beall et al. 1964). The first barrier is the salt where 100% of noble gases, 10% of the iodine, and 10% of the solid radionuclide contained with the fuel salt are released from the primary vessel into the immediate containment cell (NRC 2019). Then, from the containment cell into the reactor building, approximately 10% for each nuclide is released, then 1% from the building into the environment is assumed. Important to note is that the basis for these estimates was primarily through expert judgment as experimental data was sparse at the time. From this information, maximum, bounding source terms are estimated for a reference 1 MW design with a near-ground (no stack) release and are shown in Table 10MWt.

Table 10. MSR credible accident radionuclide release rates, in curies, adapted from ORNL report (Beall et al. 1964).

Key Radionuclide	Reference 10 MWt	Scaled to 1 MWt	Release Rate into RB (10% from Cell)	Release Rate into Environment (1% from RB)
Xe-133	2.14E+05	2.14E+04	2.14E+03	2.14E+01

Key Radionuclide	Reference 10 MWt	Scaled to 1 MWt	Release Rate into RB (10% from Cell)	Release Rate into Environment (1% from RB)
Kr-85	1.61E+03	1.61E+02	1.61E+01	1.61E-01
Kr-88	1.59E+05	1.59E+04	1.59E+03	1.59E+01
I-131	1.44E+04	1.44E+03	1.44E+02	1.44E+00
I-132	2.13E+04	2.13E+03	2.13E+02	2.13E+00
I-133	3.11E+04	3.11E+03	3.11E+02	3.11E+00
I-134	3.05E+04	3.05E+03	3.05E+02	3.05E+00
I-135	2.78E+04	2.78E+03	2.78E+02	2.78E+00
Te-129m	2.06E-01	2.06E-02	2.06E-03	2.06E-05
Te-132	5.98E+00	5.98E-01	5.98E-02	5.98E-04
Cs-134	1.03E+04	1.03E+03	1.03E+02	1.03E+00
Ag-111	6.44E+00	6.44E-01	6.44E-02	6.44E-04
Ru-103	6.44E+00	6.44E-01	6.44E-02	6.44E-04
Ru-106	3.09E+00	3.09E-01	3.09E-02	3.09E-04
Mo-99	5.98E+00	5.98E-01	5.98E-02	5.98E-04
Nb-95	4.84E+00	4.84E-01	4.84E-02	4.84E-04
La-140	5.46E+05	5.46E+04	5.46E+03	5.46E+01

Similar dispersion assumptions for GCRs are used for MSRs. A comparison to the MSR maximum credible accident (MCA) doses are shown on Figure 23.

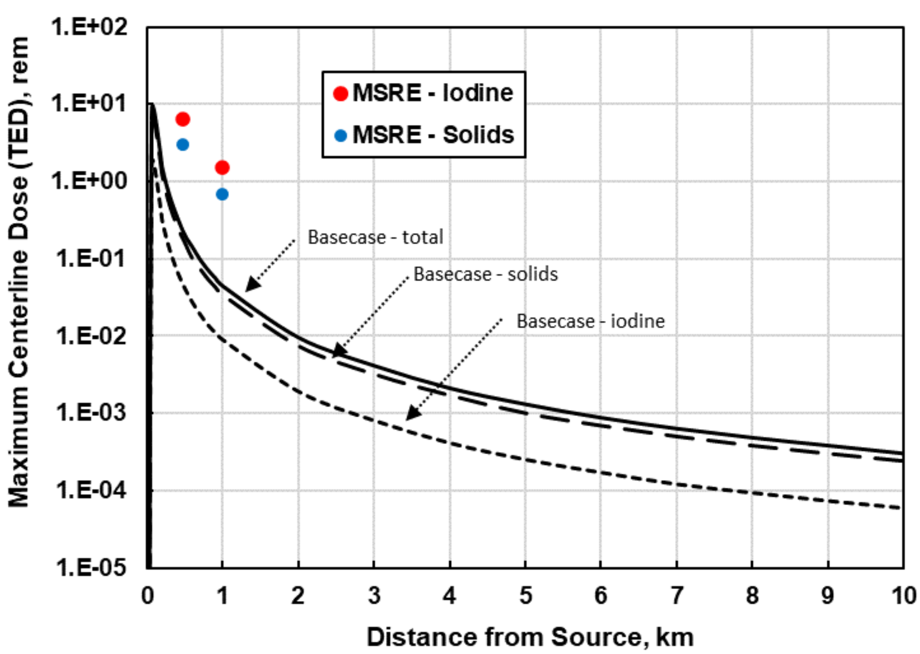

Figure 23. MSR centerline dose as a function of distance from source.

Dose rates as a function of distance from the reactor are higher than for the GCR case. This is primarily due to the retention associated with the TRISO fuel as compared to the release assumptions with the salt. MSR MCA releases are higher than the basecase [1 MWt] MSR results shown here. When comparing at 1 MWt, dose rates from solids are similar, except predicted iodine is much lower than reported for the MSR. Other than iodine, the radioisotope distribution is not reported in the MSR safety analysis but can be determined from other burnup analyses (Creasman 2020). Several other possibilities for the differences include:

- Analysis model (gaussian plume) differences associated with Hotspot as compared to the MSR safety analysis.
- Stack height.
- MCA weather conditions, wind stability, and direction.
- MCA time-dependent release characteristics to the environment from the building.

One of the mitigation systems in the MSR was a fan and filter system that sends the effluent to a 100-foot-tall stack for environmental release. This fan and filter system was assumed to have a 99.9 % efficiency. This case with a fan, filter, and 100-foot-tall stack, along with the basecase, are presented in Figure 24.

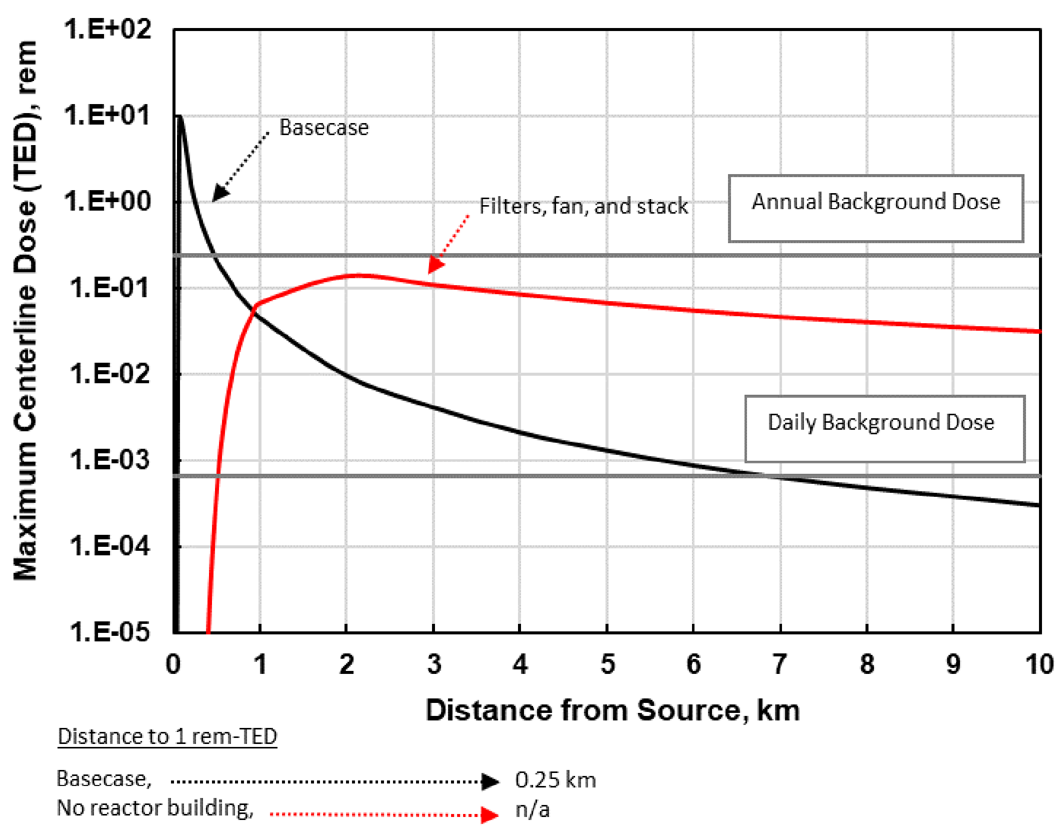

Figure 24. MSR centerline dose as a function of distance from source.

With the filters, fan, and stack, there is a trade-off between onsite and offsite releases. For the basecase, higher doses are observed immediately surrounding the facility. Use of dispersion devices is consistent with minimizing worker risks during an accident, but could result in higher offsite doses. For microreactors with small exclusion zones, offsite could be immediately near the facility. Therefore, a small stack may be beneficial to reduce the peak dose.

4.3 Heat Pipe Reactor Findings

The initial radionuclide inventories for HP reactors are different from low-assay (<5% enriched uranium) reactors. HP microreactors may employ HALEU, up to 19.75% fissile content, and use TRISO or UO2 fuel pins. As a starting point for the assessment of barrier performances, a reference UO2 inventory was selected (Southern Company 2014). The reference and scaled radionuclides used for this dose assessment are presented in Table 11.

Table 11. HP activities and release rates, in curies.

Key Radionuclide	Reference 3468 MWt	Scaled to 1 MWt	1 Barrier (0.001% leak)
Xe-133	1.90E+08	5.48E+04	5.48E-01
Kr-85	1.06E+06	3.06E+02	3.06E-03
Kr-88	7.14E+07	2.06E+04	2.06E-01
I-131	9.63E+07	2.78E+04	2.78E-01
I-132	1.40E+08	4.04E+04	4.04E-01
I-133	1.99E+08	5.74E+04	5.74E-01
I-134	2.18E+08	6.29E+04	6.29E-01
I-135	1.86E+08	5.36E+04	5.36E-01
Te-129m	4.50E+06	1.30E+03	1.30E-02
Te-132	1.38E+08	3.98E+04	3.98E-01
Cs-134	1.94E+07	5.59E+03	5.59E-02
Ru-103	1.45E+08	4.18E+04	4.18E-01
Ru-106	4.77E+07	1.38E+04	1.38E-01
Mo-99	1.84E+08	5.31E+04	5.31E-01
Nb-95	1.67E+08	4.82E+04	4.82E-01
La-140	1.82E+08	5.25E+04	5.25E-01

Like MSRs and HTGRs, the HP initial inventory is scaled to 1 MWt and then the barrier performance is applied. The barrier performance shown in the column labeled "1 Barrier (0.001% leak)" is based on the eVinci™ reactor radiological consequences in Table 2. For simplicity, the release is applied uniformly to all radionuclides. Therefore, additional barriers applied uniformly would have the same release, just scaled by the factor of the additional barrier. The resulting centerline dose as a function of distance is shown in Figure 25.

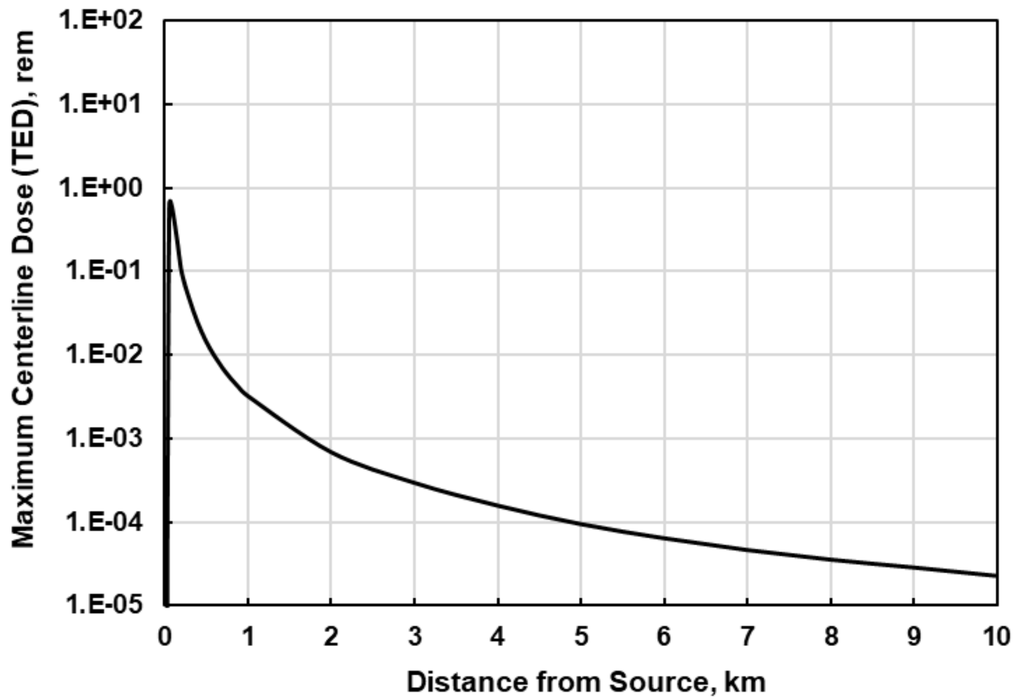

Figure 25. HP centerline dose as a function of distance from source.

Compared to the dose consequences presented in Table 2 and Table 3, this is lower by approximately a factor of 10 from “release Scenario a” described in Section 1.2.1. This is most likely due to the considerably lower reference radionuclide inventory used in this analysis. HP microreactor fuel will likely incur a much higher end-of-life burnup and have a higher FP inventory on a per-MWt basis. When this is accounted for, the HP centerline would be similar to the MSR basecase and HTGR condition with no RB.

No other unique barriers are assessed for HP reactors as barrier performances would reveal similar insights to those previously discussed for MSR and HTGR.

4.4 Dose and Barrier Analyses Discussion

Notably, the generic dose and barrier assessments in this study do not favor any microreactor design concept. Design-specific implementations could potentially net different conclusions, particularly when assumptions for the dose assessment are refined. In the present analysis, several reference radionuclide inventories were employed. These reference values are highly dependent on the core and operational conditions of those specific designs. Barrier performance values could be different than what is summarized in this study. For example, dispersion and offsite doses are sensitive to stack height and fan speed (flow rate) if they are employed. If there is not a stack or exhaust fan, release height from the ground also plays a sensitive role in the radionuclide dispersion calculations.

From Figure 24, an exhaust stack and fan reduce site dose at a 1 km or less from the reactor. However, doses farther away could be greater. At 1 MWt, this is not likely to challenge public safety. However, at 10 MWt, this could start to challenge EPA PAG limits for emergency planning.

One barrier not examined explicitly in this report is embedment or burial of a microreactor. For low pressure systems (e.g., MSRs or HP), embedment could trap some heavy noble gases and act as another filter or barrier to other volatile fission products. Embedment of a reactor operating under high-pressure may not retain as many radionuclides in the event of a break in the reactor system. From a radionuclide retention standpoint, embedment would trap fission products closer to the reactor, rather than dispersing them longer distances. For a design-specific calculation, the trade-offs between near-reactor versus offsite (e.g., > 1 km, or whatever site boundary is selected) radionuclide release should be evaluated. For autonomous, or other facilities with a minimal human presence, embedment may be preferable. Emergency planning may also be simplified where onsite evacuation may be all that is necessary to ensure safety to all populations.

An important barrier that underpins all reactor concepts is the fuel or fuel system (i.e., combined TRISO and matrix barriers, fuel salt). The assumptions on radionuclide release from the fuel in this report are highly conservative to illustrate bounding or worst-case conditions. However, design-specific values are expected to further reduce dose and potential radiological consequences.

5. INSIGHTS

5.1 Comparison Between Microreactor Technologies

Generic dose and radionuclide dispersion calculations were performed for three types of potential microreactors. These include GCRs, molten salt (liquid fuel) reactors, and HP reactors. Reference radionuclide inventories were identified and scaled to a 1 MWt design. Of the three types, no accurate reference radionuclide inventory for the HP reactor could be identified and thus a LWR UO2 profile was supplanted.

When comparing these three types of reactor designs, several insights in terms of radionuclide retention and barrier performances can be drawn. As was mentioned in Section 4.4, these insights are only with respect to the designs' generic conditions presented, rather than from any one particular design. First, even in the worst case or bounding condition, it would be highly unlikely that 1 MWt microreactors would challenge any limits on radiological release during an accident. This power level then is a sufficient "minimum" from a radiological release perspective to begin an analysis at high power levels, evaluating the trade-off between dose and economics.

Second, these high-level and generic radiological assessments seem to confirm some established perceptions of fuel radionuclide retention performance. TRISO fuel has the lowest "worst-case" or bounding release from the fuel. MSRs and HP reactors must rely on a functional containment approach that favors other barriers such as containment structures for similar safety performance. This is not an inherent disadvantage as these barriers could also be highly reliable and potentially easier to verify. Additionally, this dose and consequence analysis only assessed the worst-case condition. More probable accidents could indicate different fuel radionuclide release results. Total plant risk evaluations must consider these higher frequency accidents in addition to the beyond-design-basis, or worst-case types of accidents.

Third, the list of potential non-fuel barriers is extensive and only a small fraction of potential options was evaluated here. Not all barriers can be applied equally to all designs. For a specific design, a systematic approach should be used to evaluate potential barriers and their relationships to radionuclide retention under both design-basis and beyond-design-basis accident conditions. A stack and exhaust fan may be a benefit under some conditions while detrimental under others. Embedment has a similar trade-off and may be more beneficial for those designs with a higher degree of automation and fewer human operators.

Finally, the dose and barrier analyses presented here did not consider other design and operational aspects such as transportation, process heat application and other collocated hazards, extreme external hazards, and other conditions that could accentuate the consequences by amplifying any release from the fuel, which was assumed as a static parameter.

The worst-case or bounding radionuclide release evaluation is only one of many factors to consider when comparing microreactor technologies. For any microreactor technology, the power level and radionuclide inventory at the time of the accident are major components of the risk and safety evaluation.

5.2 Trade-offs and Relationships

Hypothetical case studies are used to conceptualize the relation between risk, performance, and cost. A 10 MWt microreactor is selected as the baseline for the consequences. Higher power output microreactor consequences are linearly scaled so that a 20 MWt microreactor doubles the consequences. In this trade-off analysis, five microreactors are assumed to be collocated at one site. The case studies evaluate when an additional barrier is needed based on the number of microreactors failing. The consequences are also linearly scaled with the number of microreactors failed at the site. The study does not detail the probability of simultaneous multiple failures of microreactors at the same site. The representation of five microreactors is shown in Figure 26, where the panel on the left side represents one failed microreactor and the panel on the right shows two failed microreactors. Based on the structural enclosure's performance, the radionuclide retention capacity factor is adjusted. When the enclosure has no damage and can retain its retention capacity, the factor is assumed to be equal to 1.0. Conversely, if the enclosure sustains the worst-case damage state (i.e., LS-A), the retention capacity factor is the lowest (0.0). This means that the structural enclosure cannot retain any radionuclides because of the cracked geometry formed after a challenging event. Table 12 shows the values for adjusting the retention capacity factor for different performance levels.

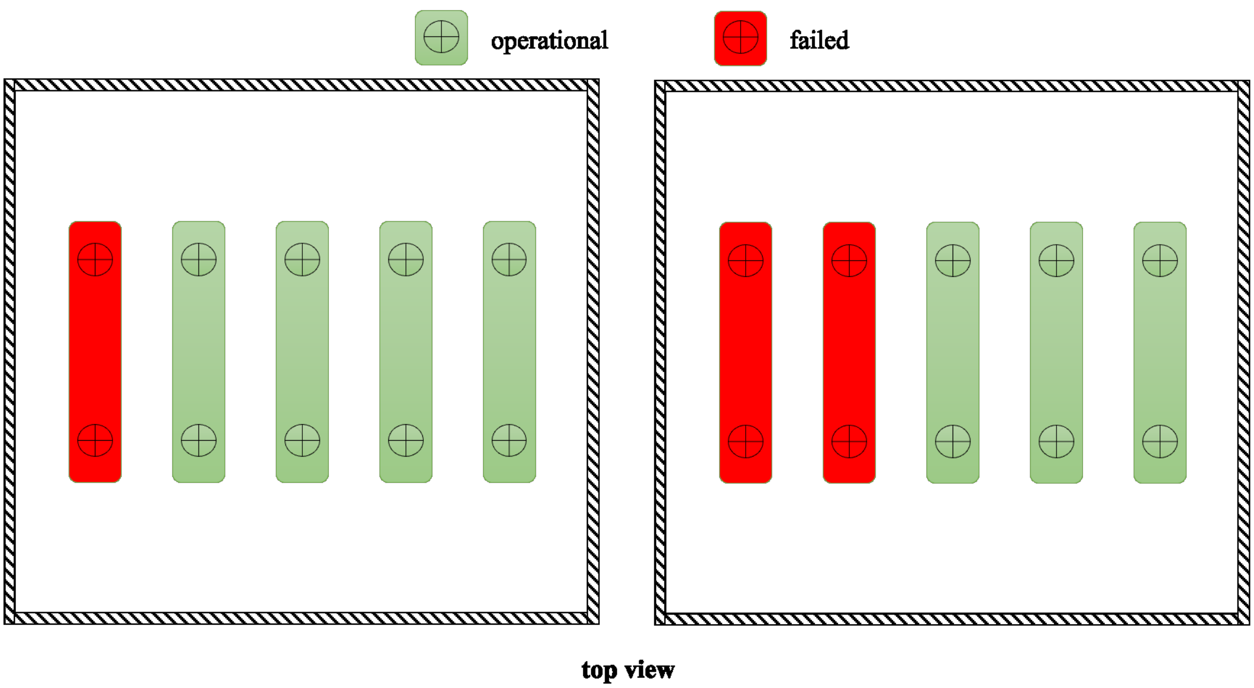

Figure 26. Schematic representation of operational and failed microreactors inside structural enclosure.

Table 12. Retention capacity factors at different performance levels.

	LS-D	LS-C	LS-B	LS-A
Retention capacity factor	1.0	0.9	0.5	0

10 MWt Microreactors

Figure 27 shows that the consequence of the high-frequency event is not challenged to remain under the curve when the containment functionality is lost. This means that the likelihood and impact are relatively low when a single microreactor fails. The microreactor package does not necessarily need additional barriers for containment. However, the figure also shows the effects on radionuclide retention if additional structural enclosure is preferred. The consequence with the additional barrier gets lower, but such an action introduces additional costs. Figure 27, Figure 28, Figure 29, Figure 30, and Figure 31 show the cases with one, two, three, four, and five microreactors failing at the same time. The consequences are linearly scaled with the number of microreactors failing. In all cases with the 10 MWt microreactors, the consequences remain under the F-C target curve. An event that triggers the failure of the microreactors may also impact the additional structural enclosure. If the enclosure is compromised under LS-A, then it is assumed to not provide additional radionuclide retention. This performance is equivalent to the case without any structural enclosure. The remaining design of the structures may provide additional retention capabilities based on their performance.

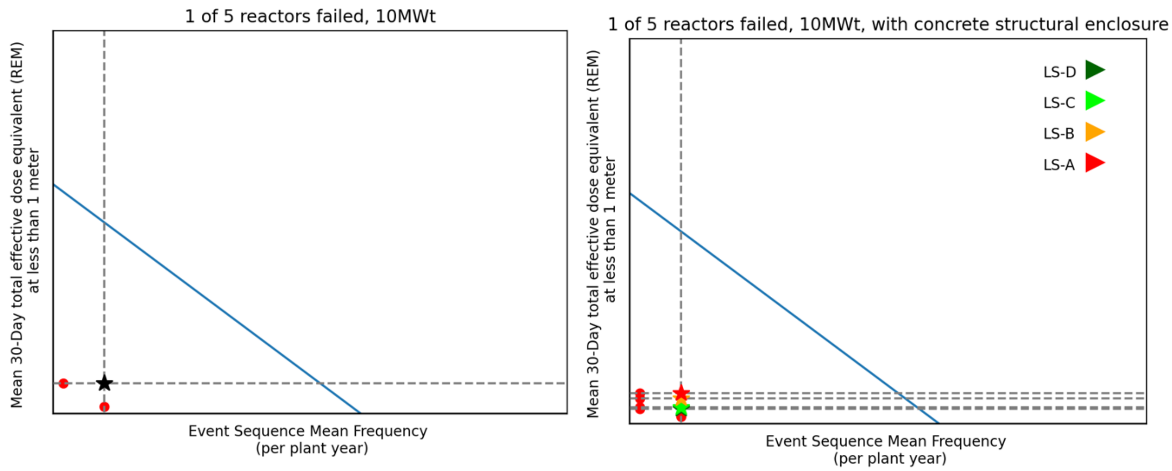

Figure 27. Single 10 MWt microreactor fail representation.

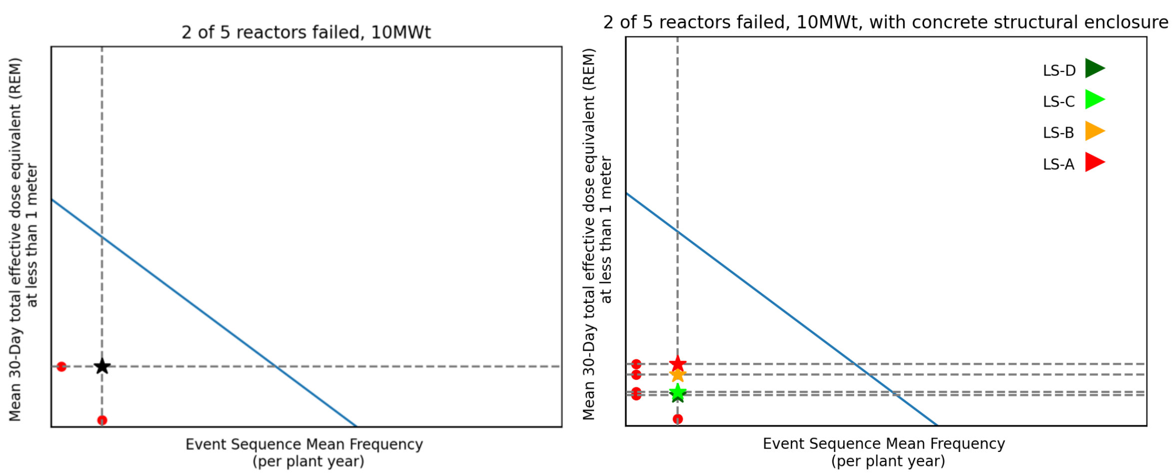

Figure 28. Two 10 MWt microreactor fail representation.

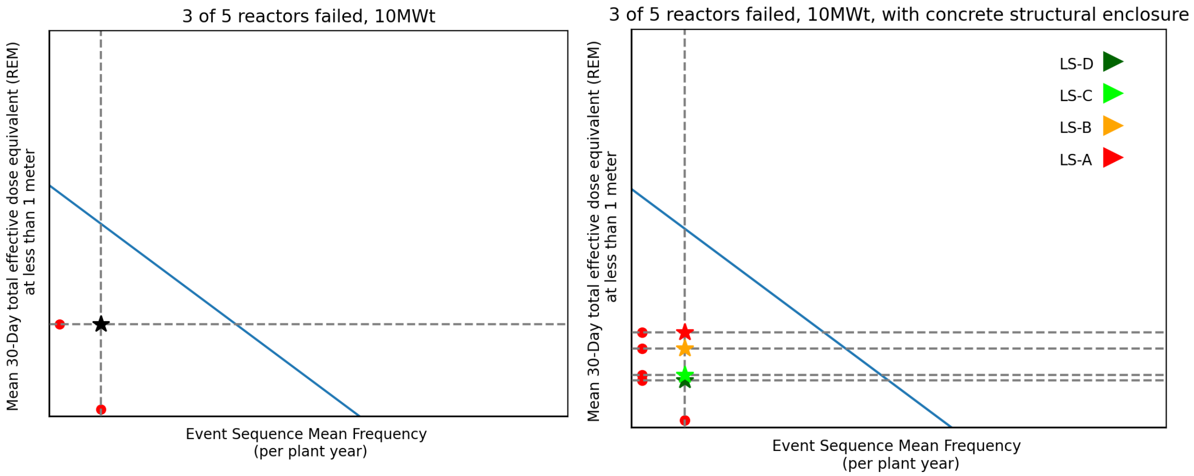

Figure 29. Three 10 MWt microreactor fail representation.

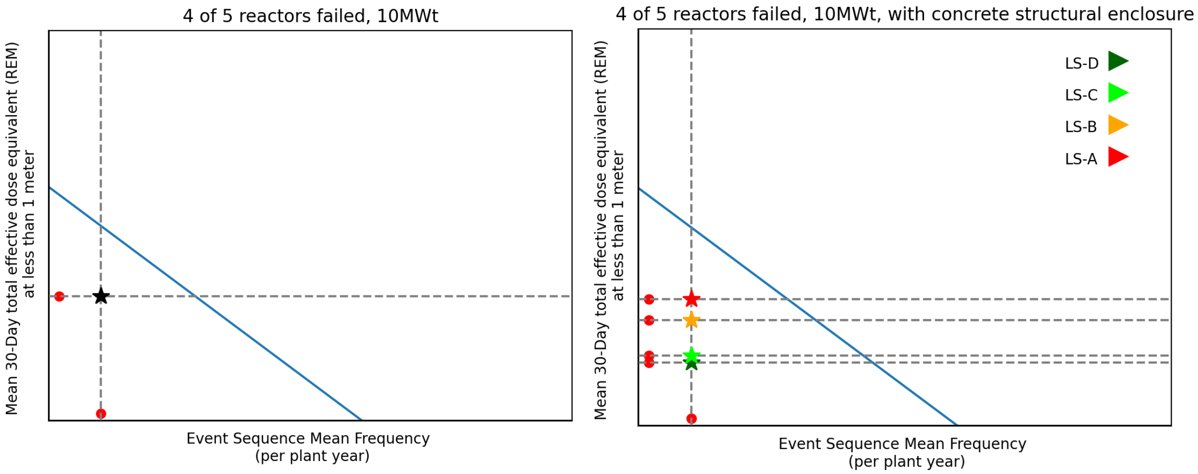

Figure 30. Four 10 MWt microreactor fail representation.

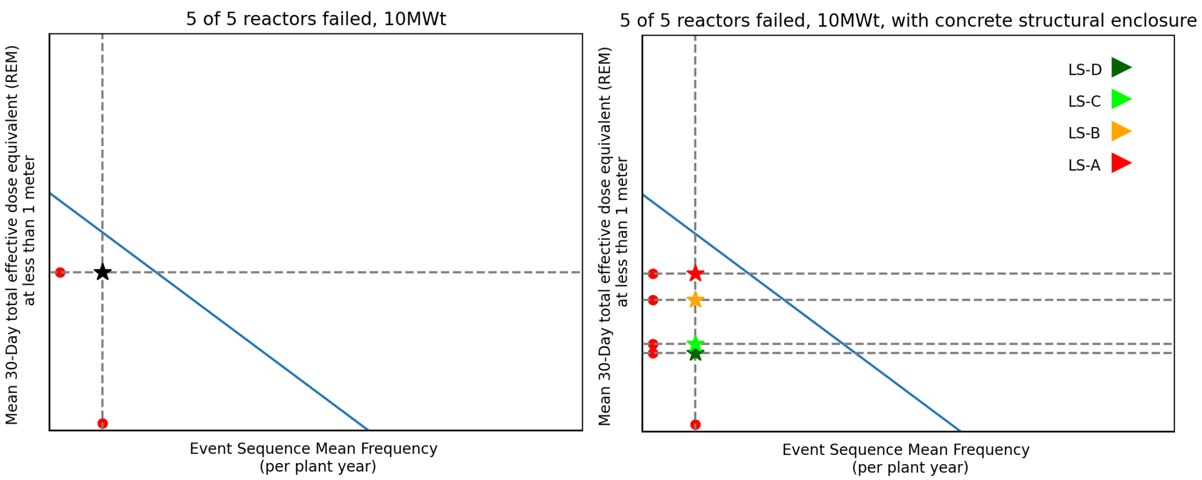

Figure 31. Five 10 MWt microreactor fail representation.

Although the 10 MWt microreactor system failure does not challenge the consequences of remaining under the target curve, the risk increases with the number of reactors failing. Designers may prefer adding an additional structural enclosure to sustain the risk under certain levels. The cost of such an additional barrier depends on the risk preference and performance expected from the additional barrier. Cost of the five 10-MWt microreactor system is the baseline for the rest of the other cases, where the output is increased between 10 and 50 MWt. Rather than working on exact cost numbers, the study provides a normalized additional cost. This is represented by *Δ*Cost/MWt, where *Δ*Cost, the cost for elastic performance (best performing) of LS-D-type structural enclosure, is normalized by the reactor thermal output. The normalized value is taken as 1.0 for the LS-D type of performance enclosure. The *Δ*Cost of the remaining structural enclosures are adjusted based on the assumptions presented in the earlier sections. Table 13 summarizes additional normalized cost for structural enclosures with different performance levels. The table also shows whether each structural enclosure helps the reactor system stay under the target curve. Green marks mean the associated structure is supporting the retention levels to stay under the curve.

Table 13. Summary of the case studies with five 10 MWt microreactors (5 x 10 MWt).

Reactor Spec.	No. of Reactors	No. of Reactors Failed	FC Target	*Δ* Cost/MWt (normalized)
LS-D	5	1		1
LS-C				0.95
LS-B				0.85
LS-A				0.75
LS-D		2		1
LS-C				0.95
LS-B				0.85
LS-A				0.75
LS-D		3		1
LS-C				0.95
LS-B				0.85
LS-A				0.75
LS-D		4		1
LS-C				0.95
LS-B				0.85
LS-A				0.75
LS-D		5		1
LS-C				0.95
LS-B				0.85
LS-A				0.75

<u>20 MWt Microreactors</u>

Figure 32, Figure 33, Figure 34, Figure 35, and Figure 36 show the cases with 20 MWt output microreactors. The consequences remain under the target curve until four microreactors fail. If the target curve is challenged as in Figure 14, the structural enclosure with LS-A performance is not considered. With four microreactors failing, only high-performance structures, LS-D and LS-C, are valuable in terms of making the consequences stay under the target curve. The enclosure with LS-B is still not providing the necessary retention levels for the system to stay under the target curve. Similarly, only LS-D and LS-C type structures are resilient enough to sustain the consequences under the target curve. However, the risks may be high for such a system to be deployed with confidence.

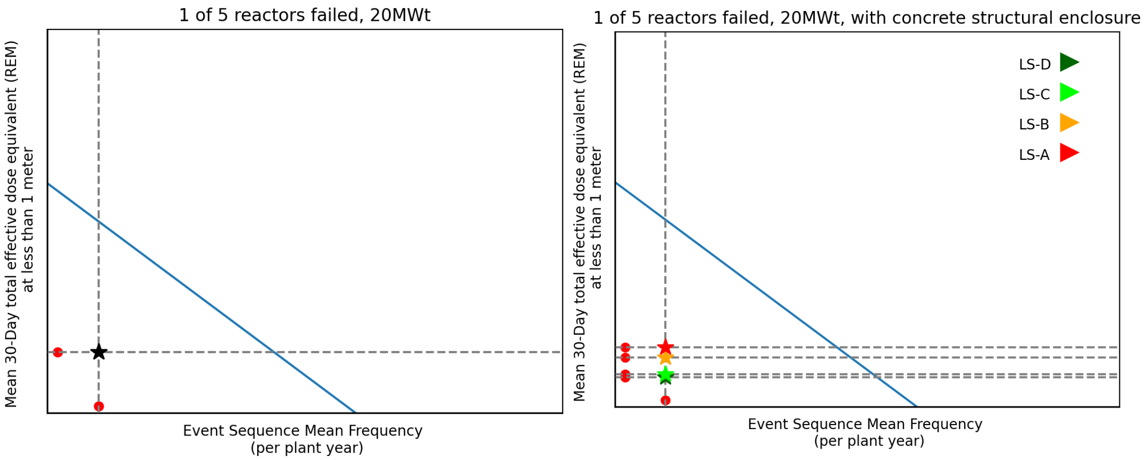

Figure 32. Single 20 MWt microreactor fail representation.

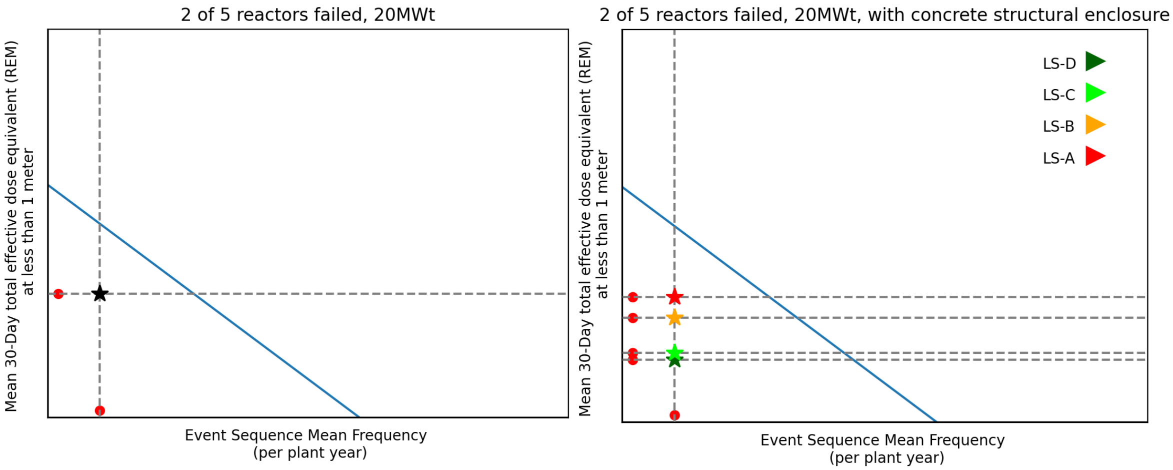

Figure 33. Two 20 MWt microreactor fail representation.

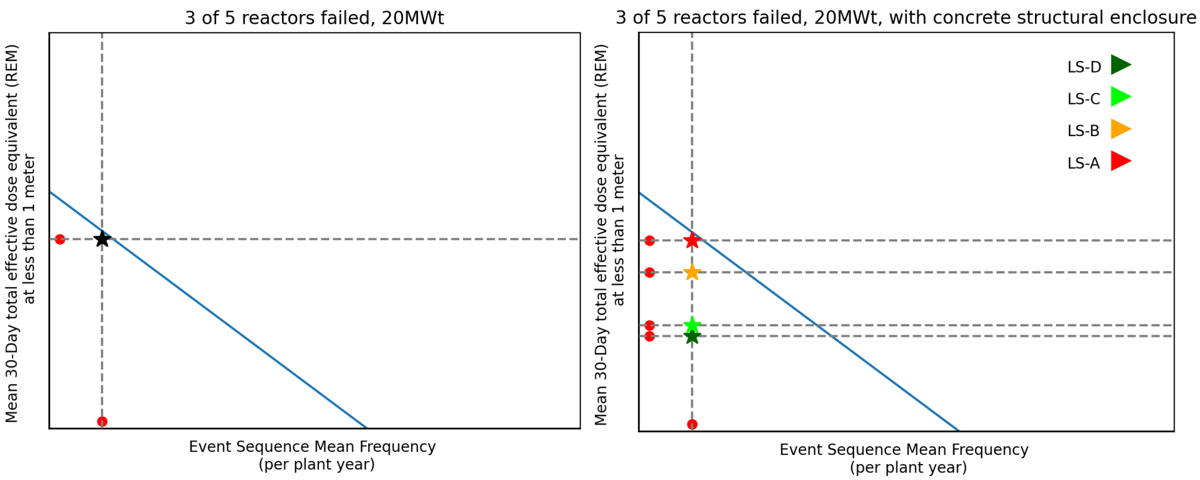

Figure 34. Three 20 MWt microreactor fail representation.

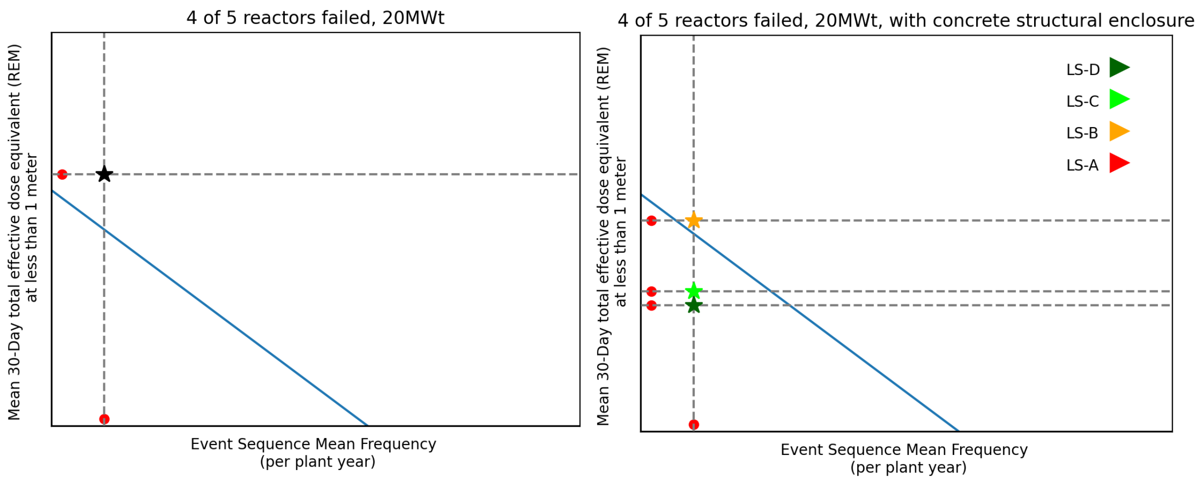

Figure 35. Four 20 MWt microreactor fail representation.

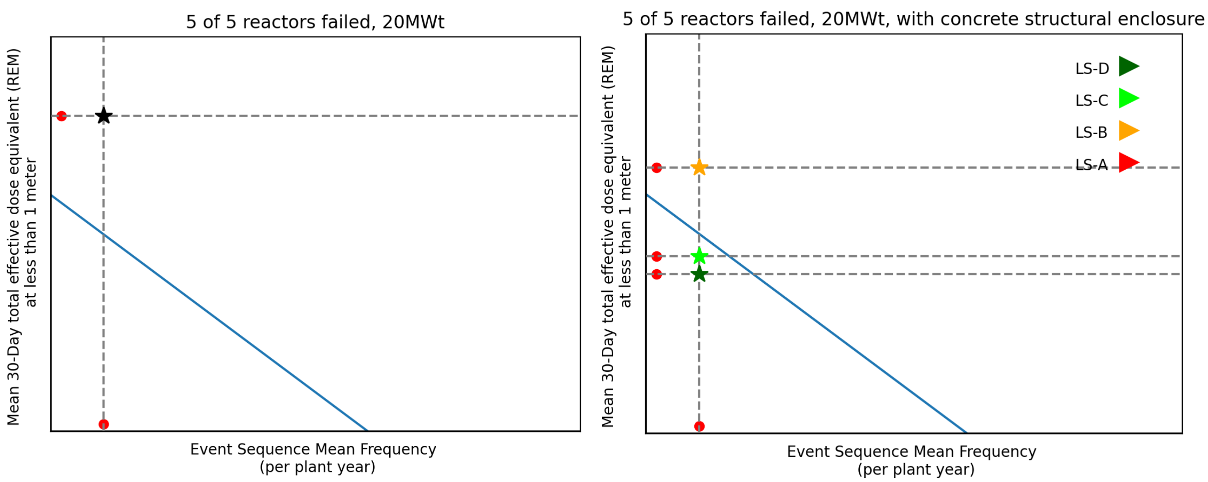

Figure 36. Five 20 MWt microreactor fail representation.

Table 14 shows the *Δ*Cost for the 20 MWt case normalized with the LS-D performance enclosure with 10 MWt reactors. As long as the consequences remain under the target curve, the differential cost is improving compared to the 10 MWt case. However, the overall risk of the system is increasing and may not produce the desired retention in case of four or five reactor failures.

Table 14. Summary of the case studies with five 20 MWt reactors (5 x 20 MWt).

Limit State	No. of Reactors	No. of Reactors Failed	FC Target	*Δ* Cost/MWt (normalized)
LS-D	5	1		0.5
LS-C				0.48
LS-B				0.43
LS-A				0.38
LS-D		2		0.5
LS-C				0.48
LS-B				0.43
LS-A				0.38

Limit State	No. of Reactors	No. of Reactors Failed	FC Target	Δ Cost/MWt (normalized)
LS-D		3		0.5
LS-C				0.48
LS-B				0.43
LS-A				0.38
LS-D		4		0.5
LS-C				0.48
LS-B				—
LS-A				—
LS-D		5		0.5
LS-C				0.48
LS-B				—
LS-A				—

30 MWt Reactors

Figure 37, Figure 38, Figure 39, Figure 40, and Figure 41 show the cases with 30 MWt output microreactors. A robust additional barrier supports the overall microreactor system consequences to remain under the FC target curve for the 30 MWt microreactors. However, the additional barrier cannot help maintain the consequences to remain under the curve after an event that results in simultaneous failure of five microreactors. The risks are getting relatively higher after three microreactor failures that the designers may need to consider additional barriers or safety systems for such situations. Table 15 shows incremental cost for different cases.

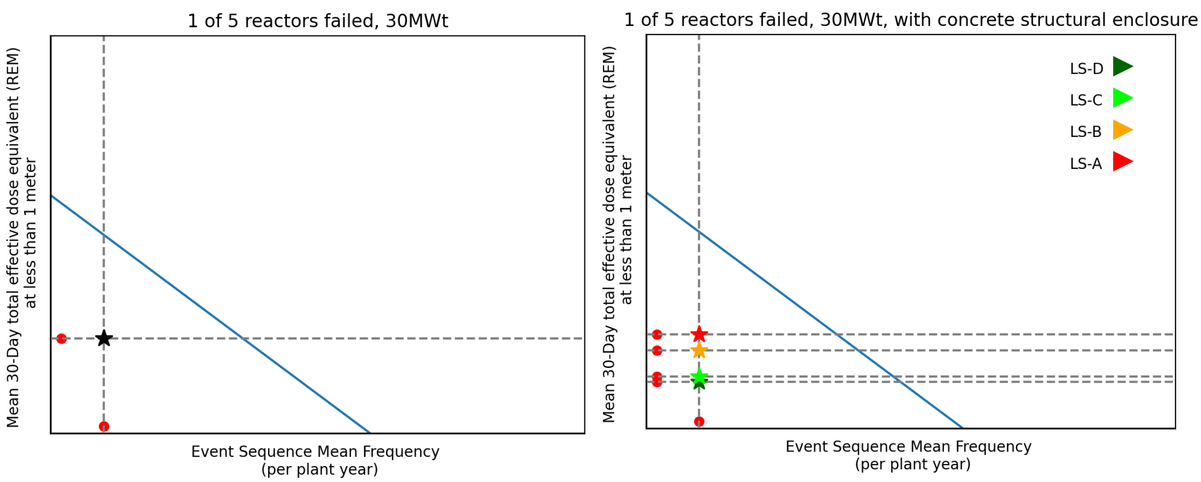

Figure 37. Single 30 MWt microreactor fail representation.

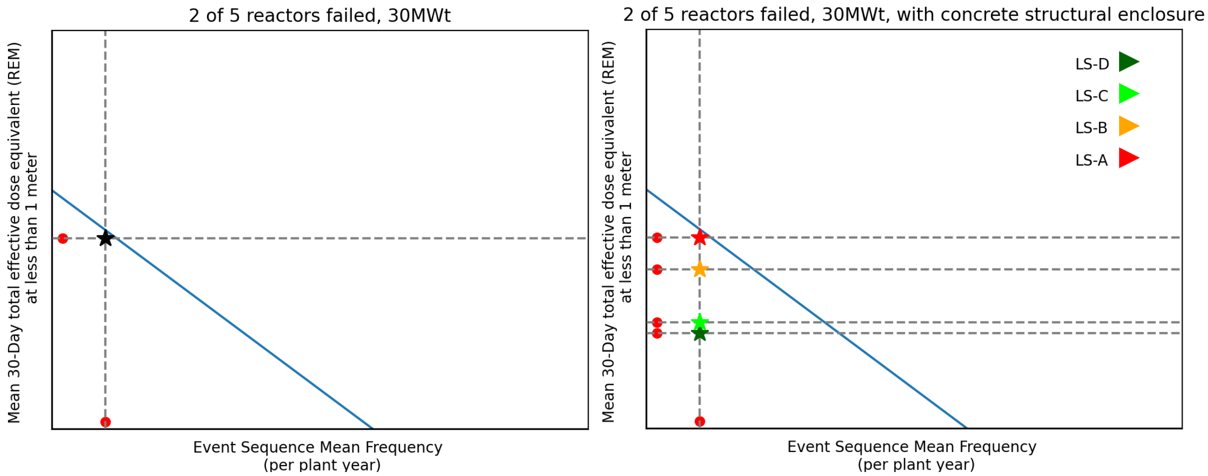

Figure 38. Two 30 MWt microreactor fail representation.

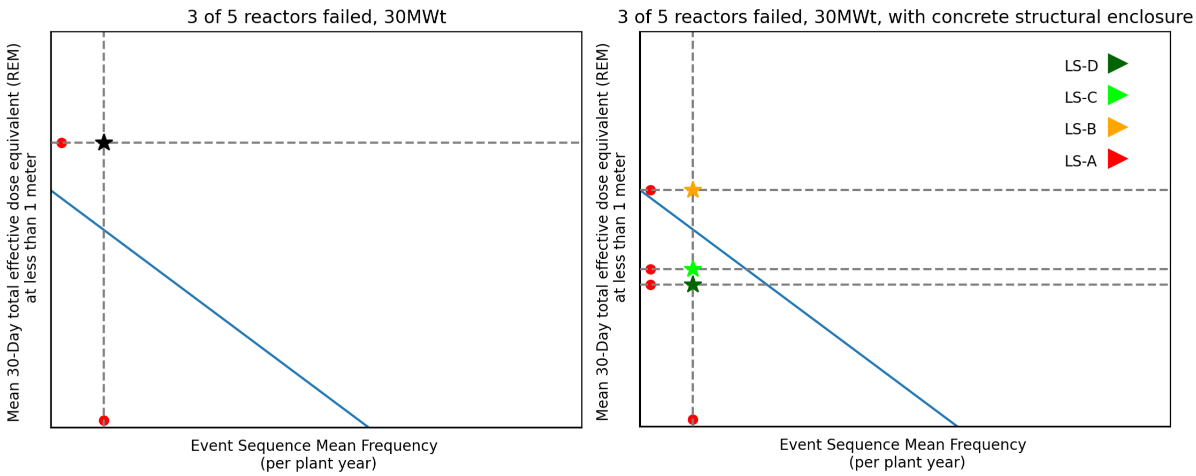

Figure 39. Three 30 MWt microreactor fail representation.

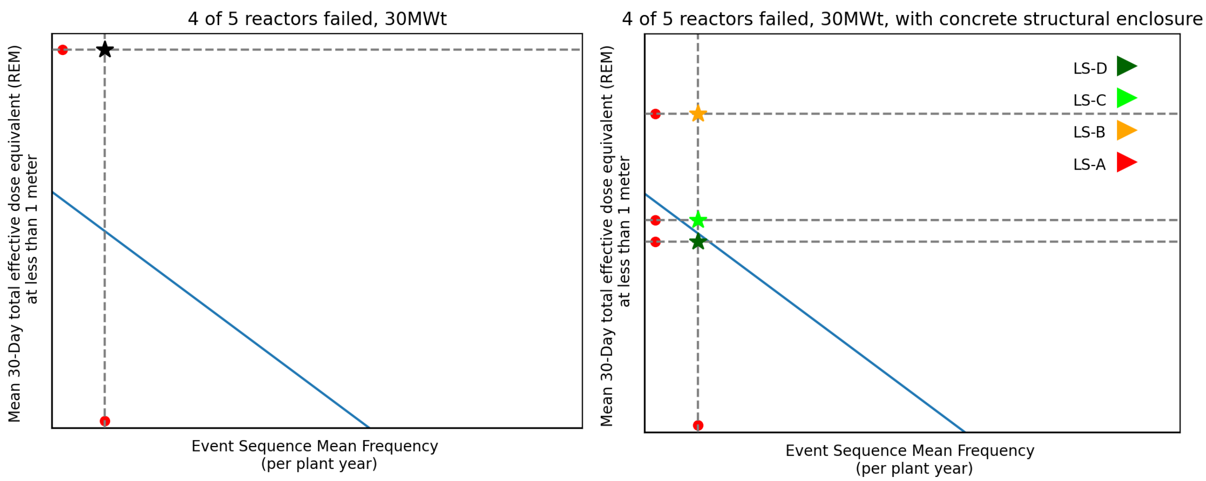

Figure 40. Four 30 MWt microreactor fail representation.

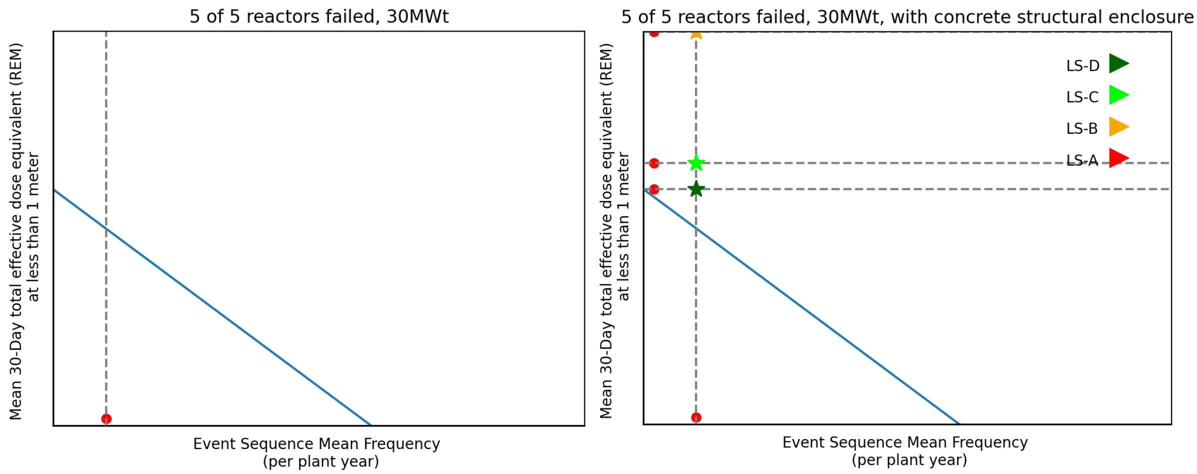

Figure 41. Five 30 MWt microreactor fail representation.

Table 15. Summary of the case studies with five 30 MWt microreactors (5 x 30 MWt).

Reactor Spec.	No. of Reactors	No. of Reactors Failed	FC Target	Δ Cost/MWt (normalized)
LS-D	5	1		0.33
LS-C				0.32
LS-B				0.28
LS-A				0.25
LS-D		2		0.33
LS-C				0.32
LS-B				0.28
LS-A				0.25
LS-D		3		0.33
LS-C				0.32
LS-B				—
LS-A				—
LS-D		4		0.33
LS-C				—
LS-B				—
LS-A				—
LS-D		5		—
LS-C				—
LS-B				—
LS-A				—

40 MWt Microreactors

The consequences are challenged to remain under the target curve for the 40 MWt case if there is more than a single microreactor failure. The additional barrier mitigates the consequences of a single microreactor failure to remain under the target curve. However, LS-B and LS-A types of structural performance are not helping when there are two microreactor failures. Under the circumstances of three reactor failures, only the most robust structure with LS-D type of performance is keeping the consequences to remain under the curve, with a relatively high-risk environment. Figure 42, Figure 43, and Figure 44 show the graphical representation of these cases. For the cases of four and five reactors, the consequences are not staying under the target curve even with an additional structural barrier of any type.

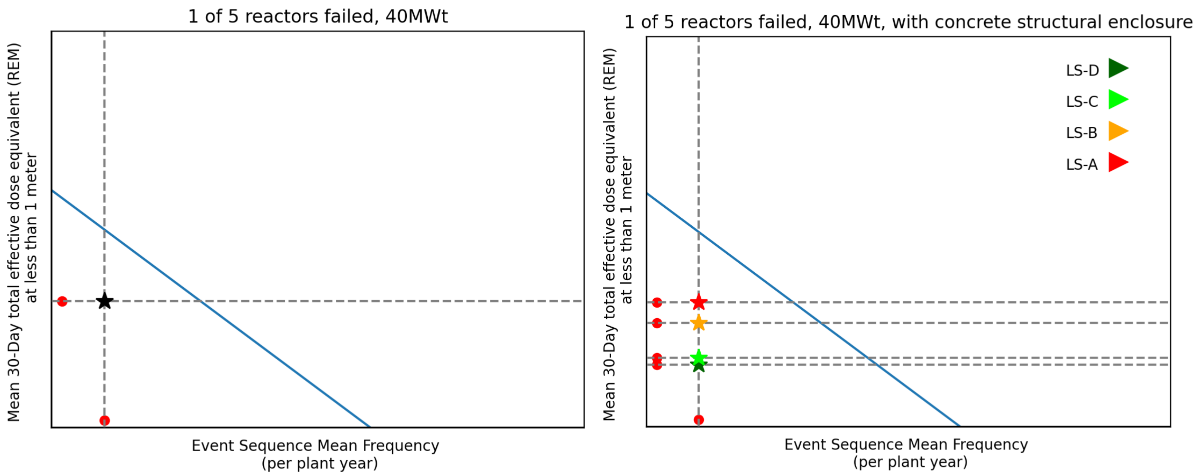

Figure 42. Single 40 MWt microreactor fail representation.

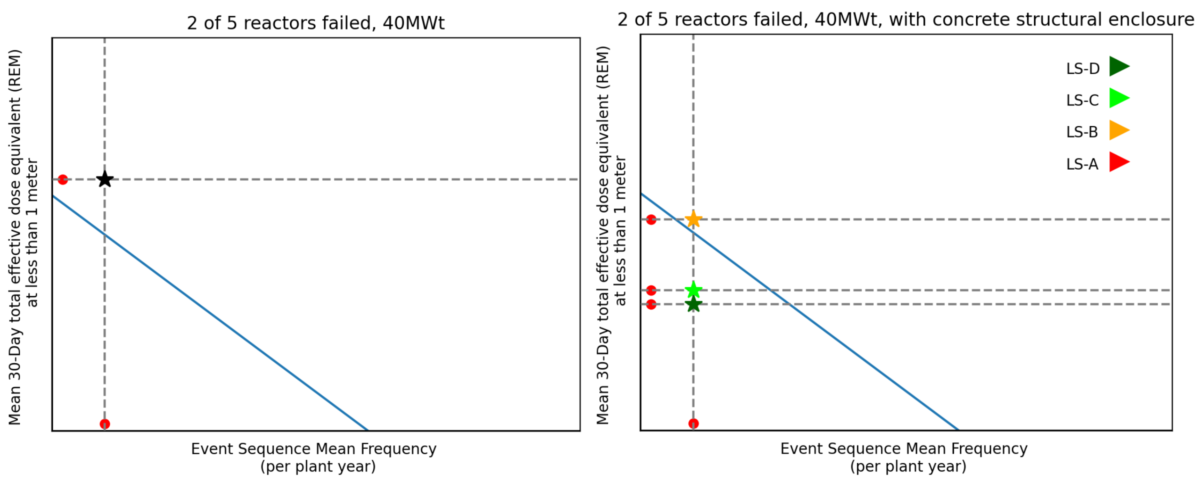

Figure 43. Two 40 MWt microreactor fail representation.

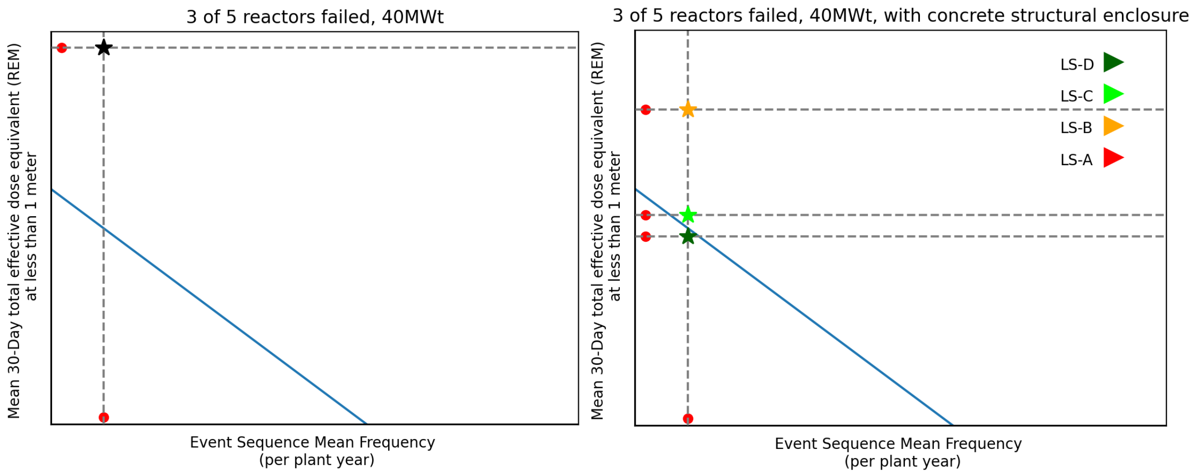

Figure 44 Three 40 MWt microreactor fail representation.

Table 16 shows the incremental cost for different cases. Cost is not considered for the cases when the additional barrier does not keep the consequences under the F-C target. For this level of power output, the strategy is to minimize the number of reactors and use relatively robust structures. The additional cost for adding the structural barriers is not a significant factor.

Table 16. Summary of the case studies with five 40 MWt microreactors (5 x 40 MWt).

Reactor Spec.	No. of Reactors	No. of Reactors Failed	FC Target	*Δ* Cost/MWt (normalized)
LS-D	5	1		0.25
LS-C				0.24
LS-B				0.22
LS-A				0.19
LS-D		2		0.25
LS-C				0.24
LS-B				-
LS-A				-
LS-D		3		0.25
LS-C				-
LS-B				-
LS-A				-
LS-D		4		-
LS-C				-
LS-B				-
LS-A				-
LS-D		5		-
LS-C				-
LS-B				-
LS-A				-

<u>**50 MWt Microreactors**</u>

If the output is increased to 50 MWt, then the system becomes risky enough not to consider deploying more than one microreactor. The additional barrier of structural enclosure supports keeping the consequences under the target curve for single microreactor. However, the risk becomes relatively high for two reactors even with additional barriers. The discussion here is having simple additional barriers—the designers may prefer deploying more complicated safety systems or barriers to keep the consequences under the target curve for two reactors. Figure 45 and Figure 46 show these two cases.

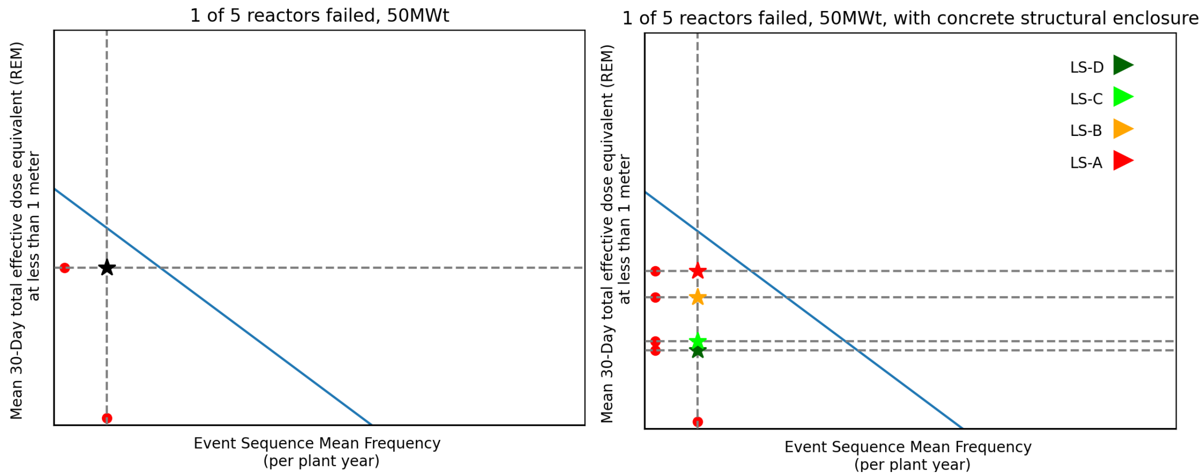

Figure 45. Single 50 MWt microreactor fail representation.

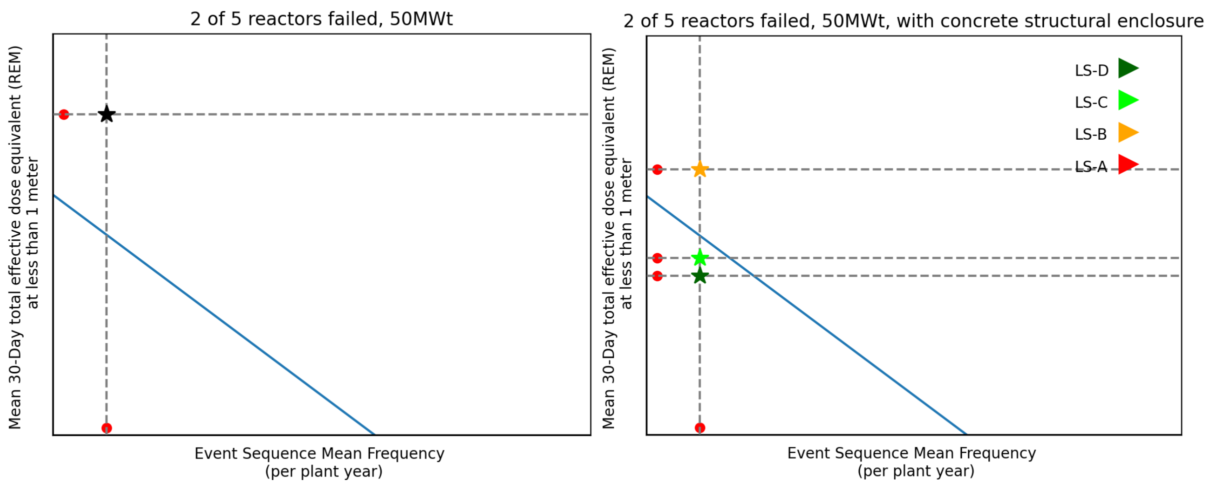

Figure 46. Two 50 MWt microreactor fail representation.

Table 17 shows the normalized additional costs for the 50 MWt microreactor case. Due to risk being higher for such outputs and five microreactors, the summary table includes the additional cost normalized for the case of a single microreactor. The economic advantage diminishes by increasing the reactor output and becomes similar to deploying five 10 MWt microreactors. The designer's choice of introducing more complicated safety systems may result in higher costs. However, more detailed analytical studies are necessary to assess the situation in real life conditions.

Table 17. Summary of the case studies with five 50 MWt microreactors (5 x 50 MWt).

Reactor Spec.	No. of Reactors	No. of Reactors Failed	FC target	*Δ* Cost/MWt (normalized)
LS-D	5	1		0.2
LS-C				0.19

Reactor Spec.	No. of Reactors	No. of Reactors Failed	FC target	*Δ* Cost/MWt (normalized)
LS-B				0.17
LS-A				0.15
LS-D		2		0.2
LS-C				0.19
LS-B				—
LS-A				—
LS-D		3		—
LS-C				—
LS-B				—
LS-A				—
LS-D		4		—
LS-C				—
LS-B				—
LS-A				—
LS-D		5		—
LS-C				—
LS-B				—
LS-A				—

In summary, this case study used simplified frequency-consequences curves to evaluate trade-offs for using an additional barrier consisting of enveloping concrete structure around the microreactor to contain fission product releases in the event of a DBE or DBA. Based on different potential damage states, the changes in the expected performance of the structures were explained in relation with existing nuclear structural codes such as ASCE-43. The damages were assumed to be in the form of cracking on the concrete structure. Increased cracking geometry was associated with lower performance levels of the structure in terms of preventing the release of radionuclides. The costs of the structures were affected by their expected performance levels after major events, such as earthquakes. The study assumed that five microreactors are collocated in a single location and enveloped with the additional barrier of a concrete structure. Without going into details of the probability of simultaneous failure of reactors, the reactors were assumed to fail in increasing numbers at the same location. A series of analyses with five output levels [10 MWt, 20 MWt, 30 MWt, 40 MWt, and 50 MWt] showed:

i) For the 10 MWt case; an additional barrier may not be necessary under progressed failure of all the reactors for the consequences to remain under the FC target.

ii) For the 20 MWt case; with the four reactors failing condition, only high-performance structures, were valuable in terms of making the consequence to stay under the target curve. Even the structures were resilient enough in sustaining the consequences under the target curve, the risks may be high for such a system to be deployed with confidence.

iii) With the remaining 30, 40, and 50 MWt reactors, the consequences were always challenged to remain under the target curve with three or more reactors failing.

iv) As can be expected, the additional normalized cost arising from introducing a new barrier gets lower with the higher output of the reactors. However, the associated risks with increased output levels may hinder their colocation. In terms of acceptable risk, cost and performance, the preferred deployment range can be between 10–30 MWt with high-performance structures, depending on acceptable risk.

6. CONCLUSIONS

This study provides background on performance-based and risk-informed design approaches for the next-generation nuclear energy technologies that enable use of a combination of different options resulting in different costs and associated risks. The study suggests that cost savings on advanced reactors may be achieved through design strategies that employ proven modularity concepts along with functional containment to create flexible designs.

Different microreactor technologies are analyzed and assessed based on their safety systems, release fractions, and radionuclide release rates. Generic dose and radionuclide dispersion calculations were performed for GCRs, molten salt (liquid fuel) reactors, and HP reactors. For all technologies at very small capacities, e.g., 1 MWt, the microreactors would be unlikely to challenge any limits on radiological release during an accident. GCRs using TRISO fuel have the lowest "worst case" or bounding release from the fuel. MSRs and HP microreactors can particularly benefit from using a functional containment approach to improve safety performance. A systematic approach is recommended for further evaluation of microreactor specific conditions to determine potential benefits from various design options (e.g., stack and exhaust fans, embedment).

A case study was performed to evaluate the risk, performance, and cost trade-offs for colocation of five microreactors at one site sharing a common barrier/enclosure structure. The analysis was performed using a range of reactor capacities from 10 to 50 MWt. The results showed that as reactor capacities were increased, high-performance structures were increasingly necessary to stay within safety limits. However, the normalized delta cost per MWt decreases as microreactor capacity increases.

This scoping study provides perspectives on how emerging regulations may interact with the economics, risk, and performance of microreactors. The study focuses on microreactor applications and lays out initial analysis approaches for further research and development activities. Understanding how to optimize microreactor designs based on these interactions is needed to enable broad future deployment of these reactors over the next few decades to assist in the transition to a low-carbon economy. This study could be expanded in the future to include:

i) New methodologies of TI-RIPB from an economics perspective as topical reports to NRC based on the existing literature, codes, and standards.
ii) Investigation of composite materials for retention barriers that are both resilient to internal and external hazards and have good retention capabilities.
iii) Testing and evaluating the performance of new microreactor containment designs under multi-hazard conditions (earthquake, flood, tornado, impact and similar).
iv) Assess the cost/risk/proliferation trade-offs from using a high confinement barrier system for microreactor transport, operation, refueling, and decommissioning as an alternative to approaches using CONEX boxes and on-site reactor facilities/infrastructure.

7. REFERENCES

Abou-Jaoude, A., A. Foss, Y. Arafat, B. Dixon, 2021. "An Economics-by-Design Approach Applied to a Heat Pipe Microreactor Concept", Idaho National Laboratory, INL/EXT-21-01201.

ASCE, 2022. Seismic Design Criteria for Structures, Systems, and Components in Nuclear Facilities, ASCE 43. https://ascelibrary.org/doi/book/10.1061/asce43.

Beall, S., Haubenreich P., Lindauer R., and Tallackson J., 1964. "MSRE Design and Operations Report, Part V, Reactor Safety Analysis Report," ORNL-TM-0732, (August 1964).

Bejaoui, S., Sercombe, J., Mugler, C., & Peycelon, H. (2007). Modelling of radionuclide release from a concrete container. Transport in Porous media, 69(1), 89-107.

Black, G., D. Shropshire, K. Araújo, 2020. “Small Modular Reactor Adoptions: Opportunities and Challenges for Emerging Markets,” in: Ingersoll and Carelli (Eds.) *The Handbook of Small Modular Reactors*. Elsevier-Woodhead Publishing, Cambridge, MA.

Black, R., 2020. “Licensing of Small Modular Reactors,” in: Ingersoll and Carelli (Eds.) *The Handbook of Small Modular Reactors*. Elsevier-Woodhead Publishing, Cambridge, MA.

Black, G., D. Shropshire, K. Araújo, A. van Heek, 2022. “Prospects for Nuclear Microreactors: A Review of the Technology, Economics, and Regulatory Considerations,” American Nuclear Society Nuclear Technology Special Edition on Microreactor, Nuclear Technology, Article ID: UNCT 2118626.

Creasman, S., 2020. "Methodology for Source Term Analysis of a Molten Salt Reactor. " Master's Thesis, University of Tennessee, 2020. https://trace.tennessee.edu/utk_gradthes/5588

DOE, 2021. “Advanced Fuel Cycle Cost Basis”, Systems Analysis and Integration, INL/EXT-21-64514.

EPA, “PAG Manual: Protection Action Guides and Planning Guidance for Radiological Incidents,” EPA-400/R-17/001, (January 2017).

EPRI, 2006, Program on Technology Innovation: 10CFR50.69 Implementation Guidance for Treatment of Structures, Systems, and Components. EPRI, Palo Alto, CA: 2006. 1011234.

EPRI, 2018. Energy Technologies Brief: Full-Power Microreactor Demonstration Expands Horizons for Nuclear Energy. https://www.epri.com/research/products/000000003002014871.

EPRI, 2019, “Uranium Oxycarbide (UCO) Tristructural Isotropic (TRISO) Coated Particle Fuel Performance,” Topical Report EPRI-AR-1 (NP).

Fair, H. R., and A. J. Huning, 2021. “TCR Postulated Accident and MHA Dose Assessment,” Oak Ridge National Laboratory, ORNL/TM-2021/1917.

Ferritto, J. M. (1984). Economics of seismic design for new buildings. Journal of Structural Engineering, 110(12), 2925-2938.

Hoffman, E., A. Abou-Jaoude, A. Foss, 2020. “Improvement of ACCERT Algorithm – FY20”, System Analysis and Integration, ANL/NSE-20/28.

IAEA, n.d. “Advanced Reactor Information System” Accessed February 22, 2023. https://aris.iaea.org/.

Ingersol, D., M. Carelli, 2021. “Handbook of Small Modular Nuclear Reactors,” Elsevier. ISBN: 978-0-12-82916-2.

INL, 2012, Next Generation Nuclear Power Project, “Scoping Analysis of Source Term and Functional Containment Attenuation Factors,” INL/EXT-11-24034.

INL, 2021, “Systems Analysis and Integration: Advanced Fuel Cycle Cost Basis Report.” https://fuelcycleoptions.inl.gov/SitePages/CostBasisReport.aspx.

Kurt, E., D. Shropshire, 2022. “Advanced Nuclear Technology Cost Reduction Strategies and Systematic Economic Review, Cost Reduction Strategy #2: Design – Modularity at scale,” GIF EMWG.

LLNL, 2010. “HotSpot Health Physics Codes User’s Guide,” V2.07.1.

MIT Interdisciplinary Study (2018), The Future of Nuclear Energy in a Carbon-Constrained World, Massachusetts Institute of Technology, Cambridge MA, https://energy.mit.edu/research/future-nuclear-energy-carbon-constrained-world/.

Moe, W.L. (2018), Licensing Modernization Project for Advanced Reactor Technologies: FY 2018 Project Status Report, No. INL/EXT-18-46151-Rev000, Idaho National Laboratory, Idaho Falls, https://doi.org/10.2172/1471714.

Moe, W.L., A. Afzali (2020a), Modernization of Technical Requirements for Licensing of Advanced Non-Light Water Reactors: Probabilistic Risk Assessment Approach. United States: N. p., 2020.

Web. doi:10.2172/1700670.

Moe, W.L., A. Afzali (2020b), Modernization of Technical Requirements for Licensing of Advanced Non-Light Water Reactors (Final Project Report). United States. https://doi.org/10.2172/1700667.

NRC, 2014. "Standard Review Plan for the Review of Safety Analysis Reports for Nuclear Power Plants," NUREG-0800 (n.d.).

NEI, 2019. "Cost Competitiveness of Micro-Reactors for Remote Markets," White Paper, Nuclear Energy Institute (2019); https://www.nei. org/resources/reports-briefs/cost-competitiveness-micro-reactors -remote-markets (current as of Jan. 21, 2022).

NRC, 2018. "Applications for Nuclear Power Plants," Regulatory Guide 1.206, Revision 1, https://www.nrc.gov/docs/ML1813/ML18131A181.pdf

NRC, 2019. NRC Non-Light Water Reactor (Non-LWR) Vision and Strategy, Volume 3: Computer Code Development Plans for Severe Accident Progression, Source Term, and Consequence Analysis, ADAMS Accession Number: ML19093B404.

Shropshire, D.E, A. Foss and E. Kurt (2021). Advanced Nuclear Technology Cost Reduction Strategies and Systematic Economic Review, GIF/EMWG/2021/001, GIF EMWG, Paris.

Southern Company, 2014. "Vogtle Electric Generating Plant (VGEP) Units 3 and 4 Updated Final Safety Analysis Report – Chapter 15 Accident Analyses," ADAMS Accession No. ML14183B386.

Southern Company, 2019a. "Modernization of Technical Requirements for Licensing of Advanced Non-Light Water Reactors: Safety Classification and Performance Criteria for Structures, Systems, and Components," SC-29980-102 Rev 0.

Southern Company, 2019b. "Fluoride-Cooled High Temperature Reactor Licensing Modernization Project Demonstration," SC-29980-203.

Southern Company, 2019c. "Modernization of Technical Requirements for Licensing of Advanced Non-Light Water Reactors, Westinghouse eVinci™ Micro-Reactor Licensing Modernization Project Demonstration," SC-29980-202.

Southern Company, 2021. "Technology Inclusive Content of Application Project For Non-Light Water Reactors, X-energy Xe-100 TICAP Tabletop Exercise Report," SC-16166-201 Rev 0.

WNA, 2020. "Harmonization of Reactor Design Evaluation and Licensing: Lessons Learned from Transport," Report No. 2020/012. Accessed February 22, 2023. https://world-nuclear.org/getmedia/cb928ee3-dea9-41ed-a324-552c499f4375/Harmonization-of-Reactor-Design-(Transport)-Final.pdf.aspx

WNA, 2021. "Small Nuclear Power Reactors," Last modified on January 2023. https://www.world-nuclear.org/information-library/nuclear-fuel-cycle/nuclear-power-reactors/small-nuclear-power-reactors.aspx